Aachener Verfahrenstechnik | RWTH AACHEN UNIVERSITY

The present work was submitted to the Chair of Process Systems Engineering
Diese Arbeit wurde vorgelegt am Lehrstuhl für Systemverfahrenstechnik

Optimal Stopping of Batch Bioprocesses: A Stochastic Differential Analysis

Optimale Abbruchzeit für Batch-Bioprozesse: Eine Analyse mittels stochastischer Differentialgleichungen

Bachelor's thesis
Bachelorarbeit

presented by/von
Rafif Sulthan Ramadhan

Examiners/Prüfer:
Univ.-Prof. Alexander Mitsos, Ph.D.
apl. Prof. Dr.-Ing. Adel Mhamdi

Advisor/Betreuer:
Dr.-Ing. Eike Cramer

Aachen, July 15, 2025

Abstract

Biochemical processes are increasingly explored as sustainable alternatives to fossil fuel-based chemical production. However, the intrinsic variability of biological systems poses challenges to traditional deterministic modeling approaches. This thesis addresses these challenges by introducing stochastic differential equations (SDEs) to model the dynamics of a batch bioprocess. Specifically, this thesis investigates the batch production of malic acid using *Ustilago trichophora* under nitrogen limitation. Parameter estimation of the deterministic model is performed using experimental data, followed by the formulation of a stochastic extension with Monod-like noise terms to capture substrate-dependent fluctuations. To evaluate the practical implications of the stochastic dynamics, an optimal stopping problem is formulated that seeks to determine the optimal time to intervene in the process as the substrate nears depletion. Drawing on financial mathematics, the Longstaff-Schwartz algorithm is adapted to determine optimal stopping times under uncertainty, which in this thesis refers to the point at which the substrate in a biochemical process reaches a certain threshold. The Longstaff-Schwartz algorithm is a regression-based Monte Carlo method initially developed for pricing financial derivatives based on solving the underlying optimal stopping problem. The algorithm was applied to two sets of five thousand simulated stochastic scenarios of the batch process. The simulation results show that the algorithm yields optimal stopping times that closely match the actual times the stochastic scenarios reach the depletion point. Statistical tests confirm the similarity of the distributions, thereby validating the approach. The findings in this thesis underscore the importance of accounting for uncertainty in biochemical process modeling and demonstrate the applicability of theoretical and computational methods from financial mathematics in optimizing biochemical processes with stochastic dynamics, which extends beyond the original domain. This interdisciplinary approach paves the way for more robust and adaptive process control and optimization frameworks in process systems engineering by accounting for stochasticity. In particular, this thesis opens up new frontiers in exploring the interplay between stochastic modeling and simulation-based optimization methods, offering a foundation for risk-aware operational and control strategies.

Task Description

Modeling of (bio-)chemical processes has advanced far in the past 150 years of industrial and academic research. The field of process systems engineering (PSE) has used these models to run decision-making algorithms for complex systems based on numerical optimization. Notably, the PSE community's research is primarily restricted to deterministic models. However, real-world systems often exhibit fluctuations or otherwise uncertain behavior. A prominent example is bioreactors, where biomass growth and conversion fluctuate over time due to the microbes' sensitivity to minor changes in the environment, e.g., pH, temperature, or the presence of trace elements. While considering uncertainty is common practice in process control, other optimization tasks, including planning and design, generally do not consider stochastic processes.

This thesis aims to analyze the stochastic dynamics of (bio)chemical engineering systems using stochastic differential equations (SDEs). SDEs augment the deterministic dynamics described by established models in chemical engineering with a stochastic noise term. Critically, this noise term may have a (nonlinear) dependence on the system states or even control inputs. Of particular interest for this thesis are optimal stopping times for batch reactors with biological stochastic reactions. Specifically, this thesis will simulate the stochastic system and write and solve stochastic optimization problems for design and operation. Furthermore, the thesis applies the Longstaff-Schwartz algorithm to compute optimal stopping times of biological batch reactors. Tasks include modeling biomass growth and product conversion using SDEs and simulation using the programming language Julia.

Declaration

I hereby declare to have listed all aids used in this thesis alongside their application below. This concerns in particular software and services for language, text, and media production. I have been made aware by my supervisor of the proper and improper use of such aids in the thesis.
In this thesis, I have

☐ In particular not used software and services for language, text, and media production.

☐ used the following aids (Please also list how you applied each aid):

Chapter	Tool(s) used	Reason for use
1	ChatGPT, Grammarly	G, A, U
2	ChatGPT, Grammarly	G, A, U
3	ChatGPT, Grammarly, Github Copilot	G, A, U, CD
4	ChatGPT, Grammarly, Github Copilot	G, A, U, CD, An
5	ChatGPT, Grammarly	G, A, U

Ort, Datum

Unterschrift

Erklärung

Ich erkläre mich hiermit einverstanden, dass die vorliegende Arbeit in der Lehrstuhlbibliothek aufbewahrt wird und kopiert werden darf und habe keine Einwände gegen eine Veröffentlichung der gesamten Arbeit oder von einzelnen Teilen daraus.

Ich bin damit einverstanden, dass die RWTH Aachen folgende Daten zu meiner Person im Internet veröffentlicht: Name, Vorname, Titel der Arbeit.

Mir ist bekannt,

- ☐ dass ich diese Einwilligung jederzeit schriftlich mit Wirkung für die Zukunft widerrufen kann und meine elektronisch gespeicherten Daten unverzüglich gelöscht werden müssen und

- ☐ die Aachener Verfahrenstechnik bei Widerruf meiner Einwilligung verpflichtet ist, mein Werk aus der Bibliothek des Instituts/Lehrstuhls zu entfernen.

Ort, Datum	Unterschrift

Contents

1 Introduction

The growing push toward more sustainable chemical production has led to an increased focus on exploring biochemical processes as an alternative to fossil fuel-based production chains. Biochemical processes utilize the cellular activities of biomass to convert bio-based feedstocks into various products, including fuels and platform chemicals. These products play an essential role in the manufacturing of polymers and solvents [1].

Modeling of biochemical processes has seen many advancements in the field of process systems engineering (PSE) [2]. The models are then used to run decision-making algorithms based on numerical optimization. Research in this area has been limited mainly to deterministic models. Biological systems, however, are fundamentally variable and heterogeneous, as cells differ in many properties, such as cell size and morphology [3]. Biological noise can be categorized into intrinsic, extrinsic, and external noises. Intrinsic noise can be considered as an inherent stochastic biochemical process, while extrinsic noise describes cell-to-cell variations [4]. External noise is the environmental fluctuations, which can include variations in temperature or pH [5]. The noise that dominates a system depends on its size. Intrinsic noise is dominant for systems with a small number of species, such as gene networks, while the dominance of extrinsic and external noise increases with the size [6]. The study of biological noise has primarily been limited to modeling and simulating the stochastic dynamics [4, 7, 8]. The interplay between inherent noise and its effects on the dynamics of upscaled systems, such as bioreactors, is rarely discussed.

Although uncertainties and fluctuations in a system are often considered in process control, other optimization tasks, such as design and planning, do not typically account for the stochastic dynamics of a process [2]. This thesis examines the implications of considering the biological noise of biochemical processes and models the resulting stochastic dynamics using stochastic differential equations (SDEs). SDEs extend es-

tablished deterministic models to include a noise term that captures the fluctuations in a process. The modeling of the noise term is also of interest in this thesis, as process fluctuations may have a (nonlinear) dependence on process variables and inputs.

Stochastic processes have been thoroughly studied, primarily in the field of finance, as market developments are more probabilistic in nature rather than deterministic [9, 10]. This thesis aims to apply frameworks from financial mathematics to address stochastic processes in (bio)chemical engineering. This thesis explores methods used in optimization problems that incorporate the dynamics of a financial market involving financial derivatives. Financial derivatives are instruments linked to a specific commodity (e.g., stocks) to enable the trading of financial risks in their own right [11]. An example of derivatives is options, which are a contract that gives the holder the right but not the obligation to sell or buy a quantity of assets at an agreed-upon price [12]. This instrument presents a decision-making challenge, in which the holder must determine when to exercise the option to minimize risk and maximize profit. This is the idea behind an optimal stopping problem.

This thesis formulates an optimal stopping problem based on a biochemical batch process, specifically determining when a batch process should be stopped under stochastic dynamics to maximize the reward. Established frameworks from financial mathematics are then applied to the batch problem. This should provide insight into the possible advantages of modeling biochemical processes as a stochastic process rather than a deterministic process.

This thesis is structured as follows: Chapter 2 provides the theoretical background of the key concepts of stochastic differential equations and optimal stopping. The modeling approach for a biochemical process is presented in Chapter 3, along with the case study investigated in this thesis. In Chapter 4, the optimal stopping problem is formulated for the bioprocess case study. The results are then presented and discussed. The final chapter provides a summary and possibilities for future work.

2 Stochastic Differential Equations

To capture the fluctuations and uncertainties, a system can be modeled using SDEs. An SDE can be viewed as an ordinary differential equation (ODE) driven by a white noise process, which serves as the source of fluctuations. In this chapter, a brief overview of key concepts in stochastic calculus is provided, including Brownian motion and white noise, Itô calculus, and the Euler-Maruyama scheme. Afterwards, the optimal stopping problem is introduced, along with the algorithm to solve such problems.

2.1 Brownian Motion

Brownian motion, also known as the Wiener process, is a fundamental concept in the study of SDEs due to its properties and contributions to the construction of SDEs. Originally, Brownian motion is used to describe the motion of a particle on a microscopic level during a diffusive mass transport, which results from the probabilistic collisions between said particle and the particles of the medium [13]. Several realizations of Brownian motion are given in Figure 2.1.

In this thesis, the standard Brownian motion (BM) is of interest. The standard BM is defined as a stochastic process $\{B_t, 0 \leq t \leq T\}$ with the following properties [14]:

- $B_0 = 0$ and the mapping $t \mapsto B_t$ is a continuous function on $[0, T]$;
- the increments $\{B_{t_1} - B_0, \ldots, B_{t_k} - B_{t_{k-1}}\}$ are independent for any k;
- the increments are normally distributed with mean 0 and variance $t_k - t_{k-1}$: $B_{t_k} - B_{t_{k-1}} \sim \mathcal{N}(0,\, t_k - t_{k-1})$ for any k.

The independence of the increments has the consequence that the sample paths of

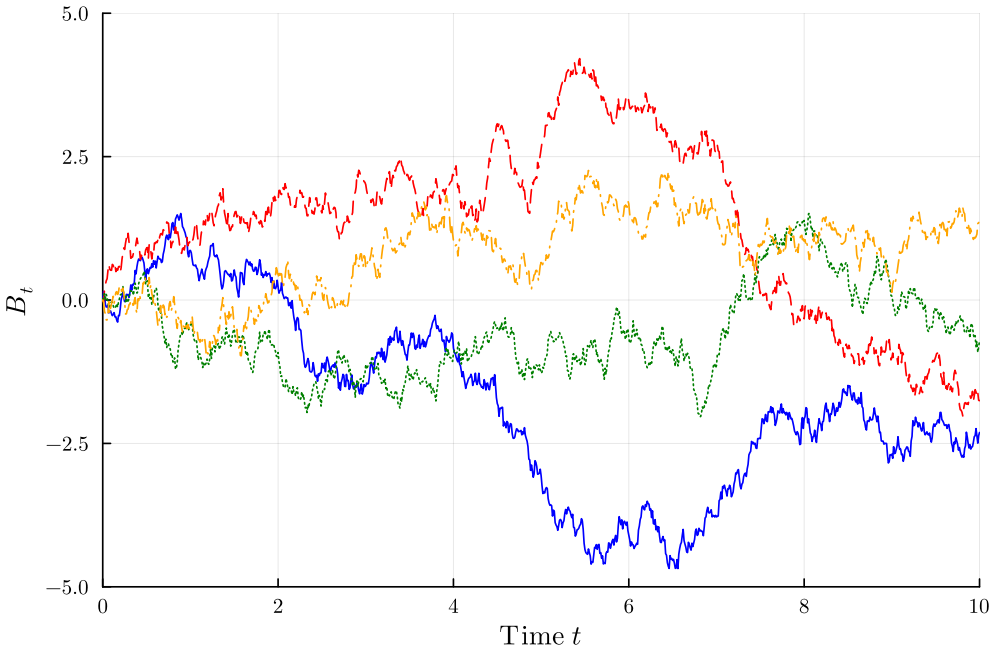

Figure 2.1: Several realizations of Brownian motion, simulated with the step size 0.01.

Brownian motion are continuous everywhere but not differentiable at any point [13]. This property is also known as the Markov property, i.e., the future value depends only on the current value [15]. Furthermore, it follows from the normal distribution of the increments and the initial value that $B_t \sim \mathcal{N}(0, t)$ for $t \in [0, T]$.

Brownian motion also serves as a prime example of a martingale, another key concept in the study of SDEs. A martingale is a stochastic process $\{M_t : t \geq 0\}$ in which the conditional expectation of the following observation is equal to the value of the current expectation, $\mathbb{E}[M_{t+1}|M_t] = M_t$. Intuitively, a martingale represents a "fair game" in the sense that the current observation is the best measure to predict the following observation. The martingale property of Brownian motion states that the expected value of future increments is always zero, i.e., $\mathbb{E}[B_{t+1} - B_t|B_t] = 0$. For modeling purposes, it is essential to consider the noise in SDEs as unbiased and, therefore, model it based on Brownian motion, which is a martingale [13].

The connection between Brownian motion and white noise that drives the SDE is noteworthy. Brownian motion can formally be regarded as integrated white noise [13]. Stated differently, white noise can be seen as the derivative of Brownian motion. This information is helpful to understand the Euler-Maruyama scheme and the Itô integral.

2.2 Euler-Maruyama Scheme and Itô Integral

A differential equation can be rewritten as an integral equation. When working with SDEs, the challenge arises to integrate white noise, since it does not actually exist as a stochastic process [13]. For this purpose, the Itô integral is introduced. The Euler-Maruyama scheme generalizes the well-known Euler method to approximate the solution of SDEs numerically.

An SDE can be considered as an ODE driven by white noise ξ_t. We consider such a differential equation with the initial condition $X(t_0) = X_0$:

$$\frac{dX_t}{dt} = \mu(X_t, t) + \sigma(X_t, t)\,\xi_t, \tag{2.1}$$

The function $\mu(X_t, t)$ is called the drift term, and $\sigma(X_t, t)$ the diffusion term. Integrating both sides of (2.1) over the time interval $[t_0, T]$ gives:

$$X_T - X_0 = \int_{t_0}^{T} \mu(X_t, t)\,dt + \int_{t_0}^{t} \sigma(X_t, t)\,\xi_t\,dt. \tag{2.2}$$

The challenge lies in the second integral on the right-hand side of this integral equation. Särkkä and Solin have shown that integration definitions from deterministic analysis (e.g., Riemann, Lebesgue, and Steltjes integrals) fail to work on this kind of integral [16]. One way to circumvent this is to utilize the fact that white noise can be formally seen as the derivative of Brownian motion and apply an Euler-type discretization in time, specifically the Euler-Maruyama scheme, to (2.2). For two time steps t and $t + \Delta t$, the discretized form (Euler-Maruyama scheme) is given as:

$$X_{t+\Delta t} = X_t + \mu(X_t, t)\Delta t + \sigma(X_t, t)(B_{t+\Delta t} - B_t). \tag{2.3}$$

Without noise, i.e., $g \equiv 0$, this scheme is the explicit Euler method for the ODE $dX_t/dt = \mu(X_t, t)$. For $dX_t/dt = \xi_t$, the scheme results in $X_t = X_0 + B_t$, which shows that Brownian motion is integrated white noise.

Now consider the time partition $0 \leq t_0 < t_1 < \cdots < t_n = T$ with the equidistant interval lengths $\Delta t = t_i - t_{i-1}$. By applying the Euler-Maruyama scheme to each subinterval, the terminal state $X(T) = X_T$ can be calculated to be:

$$X_T = X_0 + \sum_{i=0}^{n-1} \mu(X_{t_i}, t_i)\Delta t + \sum_{i=0}^{n-1} \sigma(X_{t_i}, t_i)(B_{t_{i+1}} - B_{t_i}). \tag{2.4}$$

When considering the limit of small time steps, $\Delta t \to 0$, the first sum converges to an integral:

$$\sum_{i=0}^{n-1} \mu(X_{t_i}, t_i)\Delta t \to \int_{t_0}^{t} \mu(X_t, t)\, dt. \tag{2.5}$$

The same approach cannot be applied to the second term. The Itô integral is introduced to handle an integral with respect to Brownian motion and is defined as:

$$\int_{t_0}^{t} \sigma(X_t, t)\, dB_t = \lim_{\Delta t \to 0} \sum_{i=0}^{n-1} \sigma(X_{t_i}, t_i)(B_{t_{i+1}} - B_{t_i}). \tag{2.6}$$

With the introduction of (2.6), the solution X_T in the limit of small time steps is:

$$X_t = X_0 + \int_{t_0}^{T} \mu(X_t, t)\, dt + \int_{t_0}^{t} \sigma(X_t, t)\, dB_t. \tag{2.7}$$

The integral equation (2.7) is commonly written in the differential form:

$$dX_t = \mu(X_t, t)\, dt + \sigma(X_t, t)\, dB_t. \tag{2.8}$$

In this thesis, SDEs are expressed in the form given in (2.8), following the standard convention in the literature. An important difference to (2.8) is that the analyzed SDEs in this thesis have time-independent drift and diffusion terms, i.e., they are only dependent on the state variable

$$dX_t = \mu(X_t)\, dt + \sigma(X_t)\, dB_t. \tag{2.9}$$

These SDEs constitute a special class of process called the Itô diffusion [17]. The state variable X_t of an Itô diffusion satisfies the Markov property, which means that estimating the future value can be done on the basis of the present variable value [17].

The leading illustrative example of an SDE is the Brownian motion with drift. A stochastic process X_t is a Brownian motion with drift μ and diffusion coefficient σ^2

(abbreviated $X \sim BM(\mu, \sigma^2)$) if it solves the SDE [14]:

$$dX_t = \mu\, dt + \sigma\, dB_t. \tag{2.10}$$

For $\mu = \sigma = 1$ starting at $X_0 = 0$, several possible realizations of (2.10) are given in Figure 2.2. It is shown that, from a single set of parameters, multiple trajectories can be obtained from the SDE (2.10). Another important example is the geometric Brownian motion (GBM), which is the most fundamental model of an asset's value in finance [14]. A stochastic process X_t is a GBM if $\log X_t$ is a BM; essentially, a geometric Brownian motion is an exponentiated Brownian motion. The following SDE describes a GBM:

$$dX_t = \mu\, X_t\, dt + \sigma\, X_t\, dB_t\,, \tag{2.11}$$

where μ, σ are known constants. A process that follows (2.11) can be abbreviated to $X \sim GBM(\mu, \sigma^2)$ [14]. Several realizations of $GBM(0.05, 0.15^2)$ are given in Figure 2.3. It is noteworthy that only one scenario (green) exhibits an exponential trend, while the others fluctuate randomly without a discernible pattern. This observation highlights the random nature of processes when subjected to noise, which is the primary reason why a noisy process must be modeled as such, rather than approximated by a deterministic model.

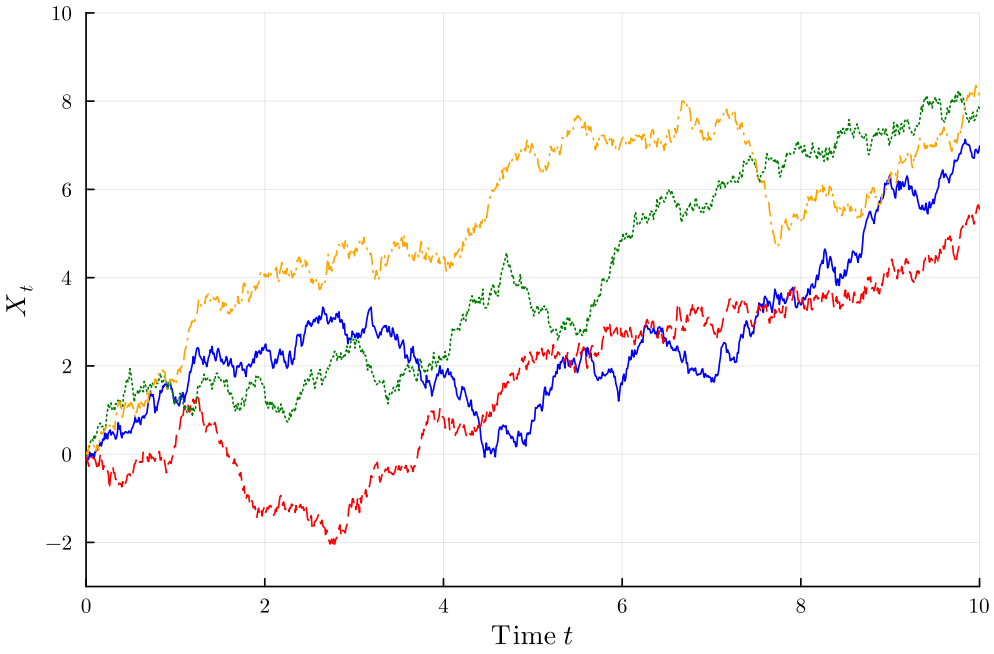

Figure 2.2: Several scenarios of Brownian motion with drift (2.10).

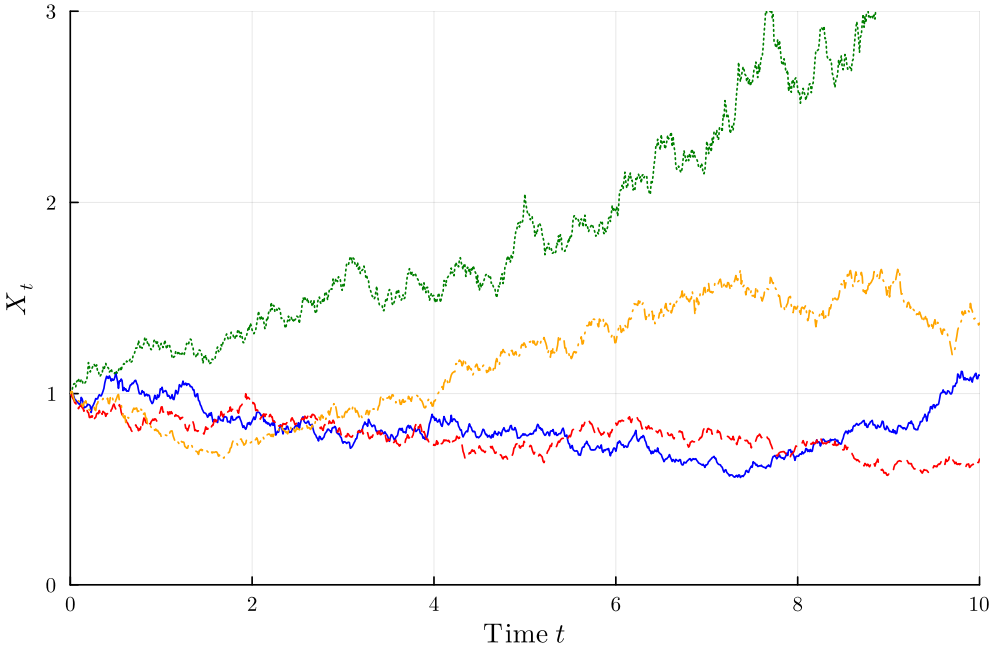

Figure 2.3: Several scenarios of geometric Brownian motion (2.11).

2.3 Optimal Stopping

This thesis investigates the optimal stopping strategy for a batch reactor, whose dynamics are subject to uncertainty and therefore modeled as a stochastic process. The optimal stopping problem is commonly found in financial mathematics, especially when working with financial derivatives or options [14]. This section provides background on optimal stopping problems in financial mathematics and the Longstaff-Schwartz algorithm, which is used initially to determine the value of options by investigating the optimal exercise strategy.

2.3.1 Motivation

To better understand the optimal stopping problem in finance, a short introduction to financial derivatives is needed. Financial derivatives are instruments linked to a specific commodity (e.g., stocks) to enable the trading of financial risks in their own right [11]. An example of derivatives is options, which are a contract that gives the holder the right but not the obligation to sell (put) or buy (call) a quantity of assets at an agreed-upon strike price K with a certain maturity date [12]. A prime example of

an optimal stopping problem is the optimal exercise strategy and valuation of options with American-style exercise features, commonly referred to as American options. The option holder has the right to exercise an American option at any time before maturity. This exercise feature presents a challenge to their exercise strategy. The payoff h_t, also known as the intrinsic value of an option, from exercise at time t is given as

$$h_{t,put} = (K - S_t)^+ = \max\{(K - S_t), 0\}, \tag{2.12}$$

$$h_{t,call} = (S_t - K)^+ = \max\{(S_t - K), 0\}, \tag{2.13}$$

where S_t denotes the value of the asset (e.g., stocks) underlying the option at the time of exercise. An option is said to be 'in the money' (ITM) if its intrinsic value is greater than zero, otherwise the option is said to be 'out of the money' (OTM). The asset price is commonly modeled as geometric Brownian motion [14]

$$dS_t = \mu\, S_t\, dt + \sigma\, S_t\, dB_t, \tag{2.14}$$

where μ, σ are known constants. The optimal stopping problem answers the question "when should the option holder decide to exercise?" Due to its stochastic nature, the holder can never be certain at the time of exercise whether the decision at that time is the best option. For example, the value of an asset may still decline after the exercise of a put option, and the option holder should have waited to receive a higher profit. A stopping strategy is necessary to achieve the best long-term outcome, which maximizes the expected profit when the time value of money is taken into account.

The optimal stopping problem of an American option is also essential in the appraisal of such contracts. The value of an American option contract is dependent on its optimal exercise strategy [14]. Therefore, valuing an American option includes solving an optimal stopping problem to find the optimal exercise rule and then deriving the option value from the maximum expected payoff. Due to the time limitation imposed by the maturity date, the formulated problem constitutes a finite-horizon optimal stopping problem. The valuation process usually approximates an American option as a Bermudan option, i.e., the option can only be exercised at predetermined exercise dates up to maturity [14]. The real American option can, of course, be continuously exercised at any time before maturity. This approximation yields a discrete, finite-horizon optimal stopping problem, which is the focus of the following analysis.

2.3.2 Problem Formulation and Backward Induction

In the following, an optimal stopping problem associated with a generic SDE is presented. Afterward, the backward induction method is explained to solve the optimal stopping problem. Consider the SDE of a generic stochastic variable X_t (2.15)

$$dX_t = \mu(X_t)\,dt + \sigma(X_t)\,dB_t. \tag{2.15}$$

Shiryaev and Peskir [18] define an optimal stopping as:

$$V_* = \sup_{\tau} \mathbb{E}[G_\tau], \tag{2.16}$$

where V_* is the value function, and G_τ is the reward for stopping at time τ. The reward function G_t is given as a function of the underlying stochastic variable, $G_t = f(X_t)$. This problem consists of two parts: compute the value function V_* as explicitly as possible, and retrieve the argument τ_* at which the supremum is achieved. It must be noted that the stopping decision must be based on the available information $\mathcal{F}_\tau$ up to time τ [18]. One method that can be used to solve (2.16) is the recursive backward induction method. Specifically, the backward induction method constitutes a martingale-based approach to a discrete-time optimal stopping problem [18].

The backward induction method is a recursive algorithm that solves the optimal stopping problem (2.16) by comparing the reward from immediate stop with the expected reward from continuation based on the information available up to that time. If the immediate reward is higher, it is optimal to stop; otherwise, continue observing the process to stop at a later time. The expected reward, also known as the continuation value, is crucial in this algorithm, as the stopping decision is made on this basis.

Before diving into the continuation value, the backward induction method is first explained to illustrate why computing the conditional expectation function is essential in solving an optimal stopping problem. The analysis is restricted to a finite-horizon discrete optimal stopping problem. For this type of problem, several pieces of information are required: the underlying stochastic process, a discrete time grid, the reward function, and its value at maturity or the terminal time step.

Consider the optimal stopping problem (2.16), which, for a finite time horizon, can be

more explicitly given as [18]

$$V_n^N = \sup_{\tau \in [t_0, t_N]} \mathbb{E}[G_\tau], \tag{2.17}$$

where τ is a stopping time in the interval $[t_0, t_N]$. Consider the discrete time grid $\{t_n : 0 \leq n \leq N\}$, with the underlying stochastic process given by the SDE (2.15). The reward function is given as a function of the underlying state variable $G_t = f(X_t)$. To simplify the notations, the reward for stopping at time t_n is denoted by G_n. The backward induction method constructs a sequence $(S_n^N)_{0 \leq n \leq N}$ that essentially describes the best expected reward if the optimal strategy is followed from time t_n [18]. The backward induction can be formulated as a dynamic programming problem

$$S_n^N = G_N \qquad \text{for } n = N, \tag{2.18}$$

$$S_n^N = \max\{G_n, \mathbb{E}[S_{n+1}^N \mid \mathcal{F}_n]\} \qquad \text{for } n = N-1, \ldots, 0. \tag{2.19}$$

The sequence is constructed by comparing the immediate reward and the conditional expectation. Given the information $\mathcal{F}_n$ up to time t_n, the conditional expectation of the future sequence S_{n+1}^N at time t_{n+1} is defined as $\mathbb{E}[S_{n+1}^N \mid \mathcal{F}_n]$. In the context of finite horizon problems, the process must be stopped at the terminal time step t_N, and the value function is therefore $S_N^N = G_N$. The method proceeds to one time step backward to t_{N-1}, at which point the process can be stopped or continued. If it is stopped, then S_{N-1}^N is equal to G_{N-1}, and if continued under the optimal strategy, S_{N-1}^N takes the value of $\mathbb{E}[S_N^N \mid \mathcal{F}_{N-1}]$, which is the expected reward at the following time step given the information up to t_{N-1}. If $G_{N-1} \geq \mathbb{E}[S_N^N \mid \mathcal{F}_{N-1}]$, i.e., the immediate reward is greater than the expected reward from continuation, then the process should be stopped; Otherwise, continue to the previous time step t_{N-2}. This comparison is carried out throughout the remaining time steps. The optimal stopping time is then defined as the earliest time when the immediate reward is equal to the optimal expected value:

$$\tau_n^N = \inf\{n \leq k \leq N : S_k^N = G_k\} \qquad \text{for } 0 \leq n \leq N. \tag{2.20}$$

In summary, this method solves the optimal stopping problem (2.16) by inductively solving smaller pieces of the problem V_n^N for $n = N, N-1, \ldots, 0$. In the context of the original problem (2.16), Shiryaev and Peskir proved that $\tau_0^N \leq \tau_*$, almost surely [18]. This method also results in the general principle that if the stopping time

τ_0^N is optimal for V_0^N, then starting the observation at time $t_n \neq t_0$ and based on the information $\mathcal{F}_n$, the same stopping rule is still optimal for the problem V_n^N. This method of solution has led to the general principle of dynamic programming, often referred to as Bellman's principle of optimality [18]. Bellman's optimality principle states that "an optimal policy has the property that whatever the initial state and decisions are, the remaining decisions must constitute an optimal policy with regard to the state resulting from the first decision" [19].

What is left to compute now is the conditional expectation $\mathbb{E}[V_{n+1} \mid \mathcal{F}_n]$. One possible approach to computing the conditional expectation is to use regression from simulated scenarios, essentially solving the optimal stopping problem by simulation [14]. Several regression-based methods were proposed by Carrière [20], Tsitsiklis and Van Roy [21], and Longstaff and Schwartz [22]. This thesis focuses on the method proposed by Longstaff and Schwartz.

2.3.3 Longstaff-Schwartz Algorithm

Longstaff and Schwartz proposed an algorithm used initially to determine the value of an American option by solving the underlying optimal stopping problem [22]. In their introduction, no specific stochastic model is introduced to model the dynamics of the underlying asset; instead, only several values at predefined time steps are provided [22]. Therefore, it seems possible to generalize the use of the algorithm to other contexts, provided that the optimal stopping problem is based on a stochastic model. This thesis aims to generalize the use of the Longstaff-Schwartz algorithm to solve an optimal stopping problem related to a stochastic batch biochemical reaction. The main idea behind the Longstaff-Schwartz algorithm, also known as Least Squares Monte Carlo (LSMC), is that the conditional expectation can be estimated from the cross-sectional information obtained from Monte Carlo simulations. In this algorithm, the backward induction method is applied to determine when to terminate the process.

Longstaff and Schwartz use a least squares approach to approximate the conditional expectation. First, the underlying stochastic model is simulated to generate many possible scenarios. Stochastic process simulation essentially means solving the SDE, or even a system of SDEs, to generate various solution scenarios. Not all simulated scenarios are used at every time step for the backward induction; only ITM scenarios are utilized. This caveat constitutes the main difference between the method proposed

by Longstaff and Schwartz and the other regression-based methods. In the original context of the valuation of an American option, this means that the option has a positive intrinsic value (2.12). By filtering out OTM scenarios, i.e., those where the option's intrinsic value is zero, the conditional expectation can be more accurately estimated in the region where exercising the option is relevant [22]. It also significantly enhances the algorithm's efficiency. Numerical tests indicate that if all scenarios were to be used in estimating the continuation value, the algorithm would have needed two or three times as many basis functions to achieve the same accuracy as the estimator based only on the ITM paths [22].

In general, ITM scenarios can be interpreted as scenarios where the process fulfills the stopping criteria at the observed time step. After filtering the ITM scenarios, M possible scenarios are left and are denoted by the set $\{\omega_j\}_{j=1}^{M}$. The reward G_t at each time step for each of these scenarios can be calculated since the reward function is already defined beforehand and is a function of the simulated state variable. The conditional expectation can then be given as the linear combination of a set of basis polynomials [22]:

$$\mathbb{E}[V_{n+1} \mid \mathcal{F}_n] = \sum_{i=0}^{K} \beta_i \, \phi_i(X_n), \tag{2.21}$$

where ϕ_i are the basis functions, evaluated on the underlying state variable X_n at time t_n, K is the degree of regression, and β_i are the regression coefficients. The original method uses the first three weighted Laguerre polynomials as basis functions [22]. Other basis functions can also be used, such as unweighted Laguerre, Hermite, Legendre, or Chebyshev polynomials. Numerical tests indicate that the type of basis functions does not have a significant influence on the accuracy of the algorithm [22]. A least squares approach is used to estimate the coefficients β_i at each time step. For all paths $\{\omega_j\}_{j=1}^{M}$ at a time step t_n:

$$\min_{\beta} \|\mathbf{G}_{n+1} - \mathbf{\Phi}\beta\|^2, \tag{2.22}$$

where $\mathbf{G}_{n+1}$ is an $M \times 1$ vector of G_{n+1}, the simulated reward at the future time step t_{n+1}. The basis function matrix $\mathbf{\Phi}$ is an $M \times (K+1)$ matrix evaluated on the underlying state variable at time t_n. The entries are $\Phi_{kj} = \phi_{k-1}(X_n)$ for $k \in [1, K+1]$. The regression coefficients are stored in β, which is a $(K+1) \times 1$ vector. At a time step t_n, the immediate reward can be calculated from the simulated state variable,

and the polynomial regression estimates the conditional expectations based on the ITM scenarios at that time. Once the conditional expectations are estimated, all the necessary information is now available, and the backward induction algorithm can be applied to construct the optimal stopping rule.

Originally, the outcome of the Longstaff-Schwartz algorithm is the optimal exercise strategy of American options. The optimal exercise rule is given as "exercise the option if the underlying asset's price is now S at the time t." Figure 2.4 illustrates what a possible optimal exercise boundary for an American option can look like. In this example, an American put option with the strike price K and maturity at time T is considered. The underlying asset is modeled as $GBM(0.05, 0.15^2)$. The optimal stopping time is τ, which denotes the first time the asset price intersects with the optimal boundary. After the optimal exercise strategy is determined, the optimal expected payoff from each simulated scenario can then be calculated. The value of an option contract is then the average of the optimal expected payoffs over all simulated scenarios [14].

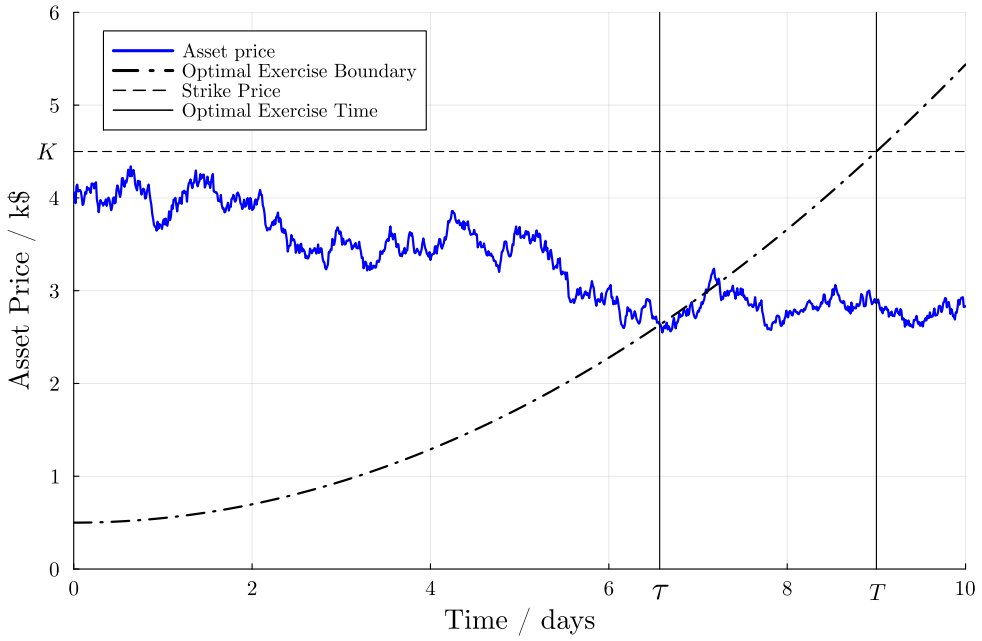

Figure 2.4: Example of an optimal exercise boundary for an American put option with strike price K and maturity at T. The optimal exercise time is τ.

3 Biochemical Process Modeling

This thesis explores the study of stochastic biochemical processes. However, such processes are generally constrained to deterministic models. This chapter first presents the background on first-principles modeling of biochemical processes. We then introduce the case study investigated in this thesis, beginning with a deterministic formulation that is subsequently extended to a stochastic model.

3.1 Biochemical Reaction

The goal of this work is to investigate an optimal stopping problem based on a biochemical process. A biochemical reaction can be generally described as:

$$\text{Biomass growth: Substrate S} \xrightarrow{\text{Biomass X}} \text{more Biomass X,} \tag{3.1}$$

$$\text{Product formation: Substrate S} \xrightarrow{\text{Biomass X}} \text{Product P.} \tag{3.2}$$

Let S, X, and P denote the substrate, biomass, and product concentrations, respectively. The most commonly used model to describe biomass growth is the Monod kinetics [23]. The Monod model relates the specific growth rate of biomass μ_X to substrate availability [24]. The mass balance of the biomass in a batch system and the specific growth rate are given as:

$$\frac{dX}{dt} = \mu_X X\,, \tag{3.3}$$

$$\mu_X = \mu_{X,max}\,\frac{S}{K_X + S}\,, \tag{3.4}$$

where $\mu_{X,max}$ is the specific growth rate and K_X is the half-saturation constant of the biomass. The half-saturation constant is the concentration at which the specific growth rate reaches half of the maximum rate. The product formation rate can also

be described using a similar equation. The product mass balance in a batch system and the specific product formation rate are given as:

$$\frac{dP}{dt} = q_P \, X \,, \tag{3.5}$$

$$q_P = q_{P,max} \, \frac{S}{K_P + S} \,, \tag{3.6}$$

where q_P and $q_{P,max}$ are the specific and maximum product formation rates, respectively, and K_P is the associated half-saturation constant. Other factors may be added to the specific rates, which include terms describing inhibition. Inhibitions can come from secondary substrates and the product itself.

The substrate is consumed by the biomass for growth and product formation. Therefore, the mass balance of the substrate must consider the different rates of consumption. For a batch reactor where the reactions (3.1) and (3.2) take place, the substrate mass balance reads:

$$\frac{dS}{dt} = \frac{-\mu_X \, X}{Y_{XS}} + \frac{-q_P \, X}{Y_{PS}} \,, \tag{3.7}$$

where the yield coefficients Y_{XS} and Y_{PS} relate the amount of substrate consumed to form more biomass and the product, respectively [23].

$$Y_{XS} = \frac{\text{Mass of biomass formed}}{\text{Mass of substrate consumed for biomass growth}} \,, \tag{3.8}$$

$$Y_{PS} = \frac{\text{Mass of product formed}}{\text{Mass of substrate consumed for product formation}} \,. \tag{3.9}$$

Possible additions to the generic model include the use of secondary substrates, which may act as a limiting substrate, and the inclusion of inhibition terms due to one of the reaction components. In this thesis, a rather complex use case is chosen as a case study: batch production of malic acid using *Ustilago trichophora* as biomass. The model includes several substrates and is inhibited by the secondary substrate and the product itself. In the next section, the deterministic model of this process is given and extended to form a set of SDEs.

3.2 Batch Production of Malic Acid

This thesis investigates an optimal stopping problem based on the batch fermentation of the platform chemical malic acid using *Ustilago trichophora* as the biomass under secondary substrate limitation due to nitrogen. For this process, the substrates sucrose, fructose, glucose, and ammonia, as the source of nitrogen, are supplied. Sucrose undergoes hydrolysis to create more fructose and glucose (monosaccharides). At the same time, the biomass grows and produces the product, malic acid. A previous work at the Chair for Biochemical Engineering by Maschmeier proposed the following model [25]:

$$\frac{dX_a}{dt} = \mu_a X_a, \tag{3.10}$$

$$\frac{dX_i}{dt} = \mu_i X_a, \tag{3.11}$$

$$\frac{dSuc}{dt} = -q_{split} X_a, \tag{3.12}$$

$$\frac{dFruGlu}{dt} = \left(q_{split} - \frac{\mu_a}{Y_{XS,a}} - \frac{\mu_i}{Y_{XS,i}} - \frac{q_P}{Y_{PS}} \right) X_a, \tag{3.13}$$

$$\frac{dN}{dt} = -\frac{\mu_a}{Y_{XN}} X_a, \tag{3.14}$$

$$\frac{dP}{dt} = q_P X_a, \tag{3.15}$$

where X_a and X_i denote the active and inactive biomass, respectively, Suc is the concentration of sucrose, $FruGlu$ is the monosaccharides fructose and glucose, N the ammonia concentration, and P the concentration of the produced malic acid. The specific growth rates μ_a, μ_i correspond to the active and inactive biomass, q_{split} describes the specific rate at which sucrose is hydrolyzed into its monosaccharides, and q_P is the specific product formation rate. The following algebraic equations give the specific rates:

$$\mu_a = \mu_{a,max} \frac{FruGlu}{FruGlu + K_{FG}} \cdot \frac{N}{N + K_N}, \tag{3.16}$$

$$\mu_i = \mu_{i,max} \frac{FruGlu}{FruGlu + K_{FG,2}} \cdot \frac{K_{IN}}{N + K_{IN}} \left(1 - e^{\frac{X_i/X_a - \phi_X}{\chi_{acc}}} \right), \tag{3.17}$$

$$q_{split} = q_{split,max} \frac{Suc}{Suc + K_S}, \tag{3.18}$$

$$q_P = q_{P,max} \frac{FruGlu}{FruGlu + K_{PFG}} \cdot \frac{K_{IN}}{N + K_{IN}} \cdot \frac{K_{IP}}{K_{IP} + \frac{w_N N}{X_a + X_i}}. \tag{3.19}$$

The initial conditions of this process from the available experimental data are given in Table 3.1.

Table 3.1: Initial Conditions for the model [25].

Component	Initial Concentration
Active biomass	1.85 $\mathrm{g/L}$
Inactive biomass	0 $\mathrm{g/L}$
Ammonia	0.762 $\mathrm{g/L}$
Sucrose	61.96 $\mathrm{g/L}$
Fructose, Glucose	12.3 $\mathrm{g/L}$
Malic acid	0 $\mathrm{g/L}$

3.3 Deterministic Parameter Estimation

The deterministic model parameters are obtained by fitting available experimental data to the model. Maschmeier previously estimated the model parameters using the pyFOOMB framework (Python Framework for Object-Oriented Modeling of Bioprocesses) [25]. However, when the model was simulated using Julia's DifferentialEquations package, the results for $FruGlu$ and P exhibited unphysical behavior, as shown in Figure 3.1. For one, upon depletion of the limiting substrate ammonia, the available fructose and glucose are consumed instantaneously, and the product concentration increases without bound, implying $dFruGlu/dt \to \infty$ and $dP/dt \to \infty$. Such gradients should be implausible, given that none of the differential equations for $FruGlu$ and P involve terms that could cause division by zero. Furthermore, the simulated profile of the inactive biomass exhibits significant deviation from the experimental data. These discrepancies indicate the need for further refinement of the parameters.

Before proceeding with the parameter estimation problem, further analysis of the system dynamics was conducted. This was motivated by the suspicion that the system exhibits stiffness, which is common for ODE systems of chemical processes [26]. The stiffness of a linear differential equation $\mathbf{y}'(x) = A\mathbf{y}(x)$ with the system matrix $A \in \mathbb{R}^{n\times n}$ and the variables $\mathbf{y}(x) \in \mathbb{R}^n$ can be measured using the stiffness ratio

$$S = \frac{\max_{1\leq j\leq n} |Re(\lambda_j)|}{\min_{1\leq j\leq n} |Re(\lambda_j)|}, \tag{3.20}$$

where λ_j $(j = 1, \ldots, n)$ are the eigenvalues of A. The system is considered stiff when $Re(\lambda_j) < 0$ and $S \gg 1$ [26].

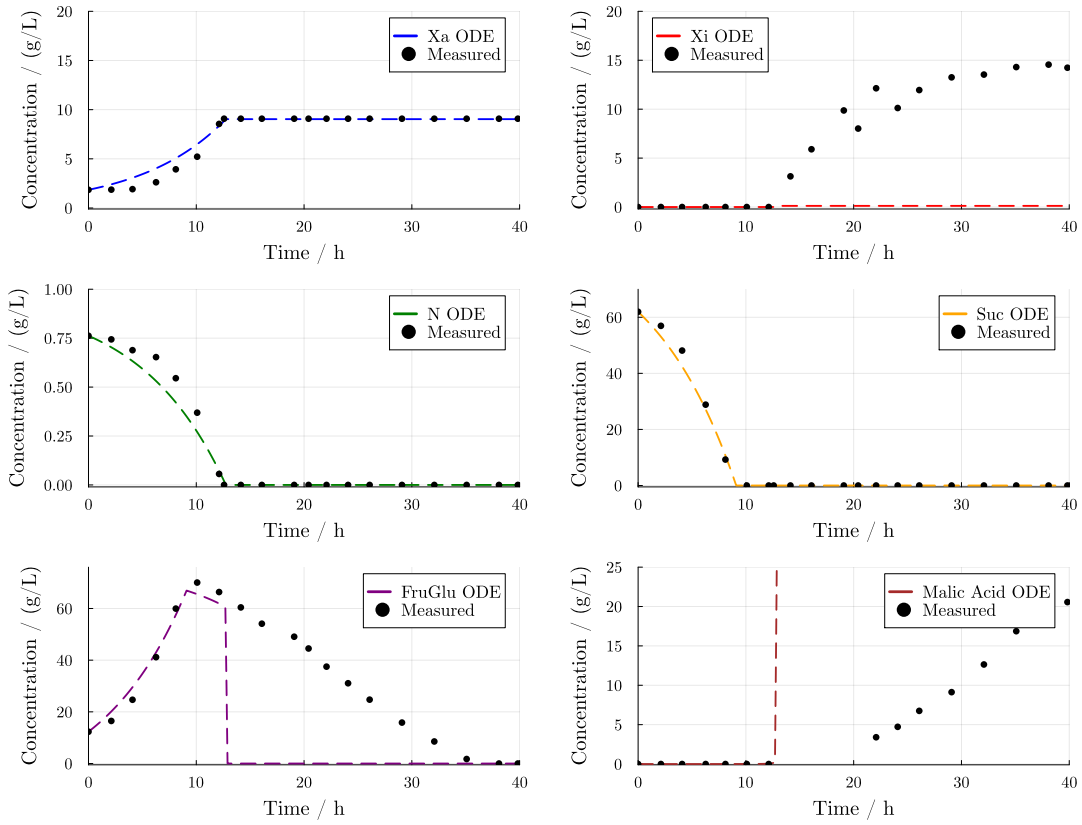

Figure 3.1: Julia simulation results using model parameters from Maschmeier [25] and the experimental data. From top to bottom, left to right: active biomass, inactive biomass, nitrogen, sucrose, monosaccharides (fructose and glucose), malic acid.

Since the system under consideration is nonlinear, $\mathbf{y}'(x) = F(x, \mathbf{y}(x))$, the stiffness can be inferred from the Jacobian matrix obtained from Taylor series linearization [27]. The results indicate that the system initially exhibits a stiffness ratio exceeding 10^5, with a pronounced fluctuation around the nitrogen depletion point. Afterward, the stiffness ratio is down to 1, indicating a non-stiff system. This ratio also corresponds to the fact that, using the original parameters, no notable development of the state variables occurs after nitrogen is depleted, as shown in Figure 3.1.

Given the system's stiffness, the selection of an appropriate numerical solver is critical. The solver Rosenbrock23 is chosen to handle the deterministic simulation following recommendations from the documentation of Julia's DifferentialEquations package. Julia provides a package to perform parameter estimation for differential equations,

the DiffEqParamEstim package. In this work, an optimization problem is formulated that minimizes the L2 loss between the data points and the predicted model. For a generic variable y, this optimization problem reads:

$$\min_{\mathbf{p}} \sqrt{\sum_{k=1}^{N_t} (\hat{y_k} - y_k(\mathbf{p}))^2}, \tag{3.21}$$

where y_k is the predicted value and $\hat{y_k}$ the data point at time t_k, N_t the amount of time steps, and $\mathbf{p}$ the parameters. The Broyden-Fletcher-Goldfarb-Shanno algorithm (BFGS) is chosen as the solving algorithm. The resulting parameters, along with those from the original work of Maschmeier, are listed in Table 3.2. For all simulations, the initial conditions are derived from the experimental data. The initial conditions are also listed in Table 3.2. The experimental data and the model fit using the optimized parameters are shown in Figure 3.2.

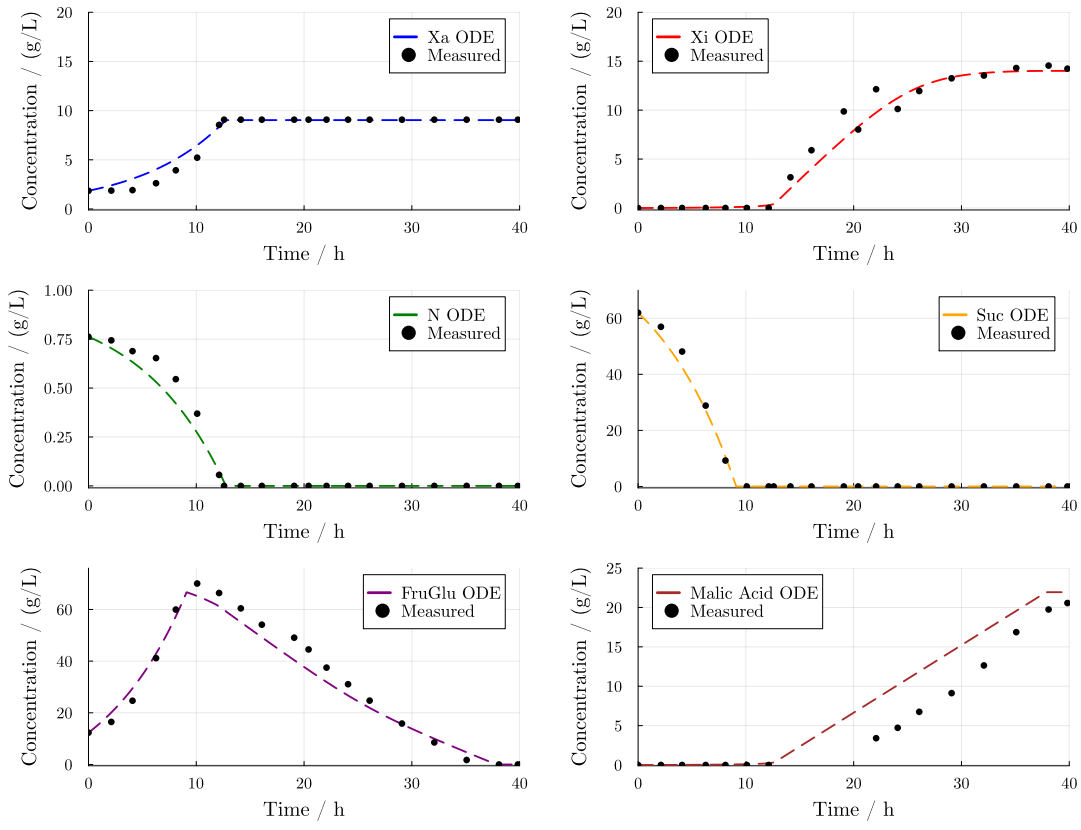

Figure 3.2: Julia simulation results using refined model parameters and the experimental data. From top to bottom, left to right: active biomass, inactive biomass, nitrogen, sucrose, monosaccharides (fructose and glucose), malic acid.

Table 3.2: Deterministic model parameters.

Parameter	Refined	Original	Unit
Max. growth rate of active biomass $\mu_{a,max}$	0.125	0.125	$1/\mathrm{h}$
Max. growth rate of inactive biomass $\mu_{i,max}$	0.125	0.125	$1/\mathrm{h}$
Max. splitting rate $q_{split,max}$	1.985	1.985	$1/\mathrm{h}$
Max. product formation rate $q_{P,max}$	**0.095**	**28.188**	$1/\mathrm{h}$
Half-saturation constant of sucrose K_S	0.00321	0.00321	$\mathrm{g/L}$
Half-saturation constant of active biomass K_{FG}	0.147	0.147	$\mathrm{g/L}$
Half-saturation constant of inactive biomass $K_{FG,2}$	3.277	3.277	$\mathrm{g/L}$
Half-saturation constant of ammonia K_N	$3.8{\cdot}10^{-5}$	$3.8{\cdot}10^{-5}$	$\mathrm{g/L}$
Half-saturation constant of product K_{PFG}	0.0175	0.0175	$\mathrm{g/L}$
Nitrogen inhibition constant K_{IN}	$\mathbf{1.47{\cdot}10^{-2}}$	$\mathbf{1.47{\cdot}10^{-4}}$	$\mathrm{g/L}$
Product inhibition constant K_{IP}	$\mathbf{1.47{\cdot}10^{-1}}$	$\mathbf{1.47{\cdot}10^{-4}}$	$\mathrm{g/L}$
Internal nitrogen mass fraction w_N	0.08	0.08	-
Acceleration factor χ_{acc}	0.3	0.3	-
Max. ratio of inactive to active biomass ϕ_X	1.56	1.56	-
Yield factor FruGlu to active biomass $Y_{XS,a}$	0.531	0.531	-
Yield factor FruGlu to inactive biomass $Y_{XS,i}$	0.799	0.799	-
Yield factor FruGlu to product Y_{PS}	0.508	0.508	-
Yield factor ammonia to biomass Y_{XN}	9.428	9.428	-

Stiffness analysis is also conducted for the newly found parameter set. Figure 3.3 shows the development of the stiffness ratio over time for both the original and updated sets of parameters. The results show that the process model is indeed a stiff system over the entire simulation time, where stark changes in the ratio can be seen around the depletion points of the substrates Suc, $FruGlu$, and N. In contrast to the behavior observed with the original parameters, the updated model exhibits an increase in the stiffness ratio following the depletion of nitrogen, indicating that the system retains its stiff character. This behavior is consistent with the dynamics of the variables $FruGlu$, X_i, and P, which now evolve at different rates. The stiffness ratio reaches a local minimum, which corresponds to the depletion of $FruGlu$.

3.4 Stochastic Process Model

The next step is to extend the deterministic model to a stochastic one by including the noise term. This noise term captures the uncertainties related to a specific parameter in the reaction kinetics. For the substrate, the noise term captures fluctuations arising

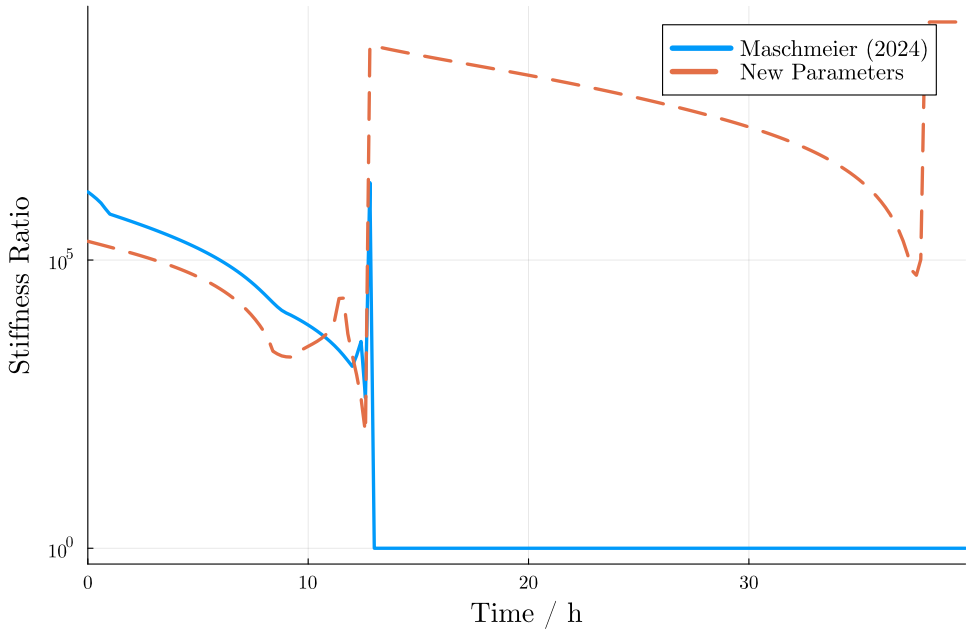

Figure 3.3: stiffness ratio over time for the original set of parameters (solid line) and for the newly found parameters (dashed line).

from the maintenance process of the biomass. The noise term in the biomass and product mass balances accounts for the noise in the reaction rates μ_X and q_P.

In biochemical processes, biomass activities are dependent on the availability of substrates. Therefore, it is assumed that the fluctuations must also follow this phenomenon. The biomass activities are expected to exhibit minimal fluctuations when the substrate is depleted and reach a saturation point when the substrate is abundant. To capture the substrate dependence, this thesis proposes modeling the noise σ_i in component i using a Monod-like equation. The Monod model is chosen because it relates microbial activities to substrate availability [24].

$$\sigma_i = \sigma_{i,max} \frac{S}{K_{\sigma_i} + S}, \tag{3.22}$$

where $\sigma_{i,max}$ is the maximum noise intensity and K_{σ_i} is the associated half-saturation constant. The variable S stands for the substrate, which can be taken by either Suc, $FruGlu$, or N. In this thesis, it is assumed that the half-saturation constant in the noise term is the same as the one used in the reaction kinetics. The model is now

given as the following set of SDEs:

$$dX_{a,t} = \mu_a \, X_a \, dt + \sigma_{X_a} \, X_a \, dB_t, \tag{3.23}$$

$$dX_{i,t} = \mu_i \, X_a \, dt + \sigma_{X_i} \, X_a \, dB_t, \tag{3.24}$$

$$dSuc_t = -q_{split} \, X_a \, dt + \sigma_{Suc} \, X_a \, dB_t, \tag{3.25}$$

$$dFruGlu_t = \left(q_{split} - \frac{\mu_a}{Y_{XS,a}} - \frac{\mu_i}{Y_{XS,i}} - \frac{q_P}{Y_{PS}} \right) X_a \, dt + \sigma_{FG} \, X_a \, dB_t, \tag{3.26}$$

$$dN_t = -\frac{\mu_a}{Y_{XN}} \, X_a \, dt + \sigma_N \, X_a \, dB_t, \tag{3.27}$$

$$dP_t = q_P \, X_a \, dt + \sigma_P \, X_a \, dB_t, \tag{3.28}$$

with the specific noise terms:

$$\sigma_{X_a} = \sigma_{X_a,max} \frac{FruGlu}{K_{FG} + FruGlu}, \tag{3.29}$$

$$\sigma_{X_i} = \sigma_{X_i,max} \frac{FruGlu}{K_{FG,2} + FruGlu}, \tag{3.30}$$

$$\sigma_{Suc} = \sigma_{Suc,max} \frac{Suc}{K_S + Suc}, \tag{3.31}$$

$$\sigma_{FruGlu} = \sigma_{FG,max} \frac{FruGlu}{K_{FG} + FruGlu}, \tag{3.32}$$

$$\sigma_N = \sigma_{N,max} \frac{N}{K_N + N}, \tag{3.33}$$

$$\sigma_P = \sigma_{P,max} \frac{FruGlu}{K_{PFG} + FruGlu}, \tag{3.34}$$

An important note in the stochastic extension of the deterministic model is that the noise in all species is generated by the BM B_t. This assumption is justified by the fact that the source of noise in a biological system is the cells or the biomass [3]. Another modeling avenue that could be explored in this regard is using independent BMs B_t^i for each species i, or introducing correlations between the different BMs.

After adding the noise terms, the concentration profiles of the stochastic system can be compared to those of the deterministic model. The maximum noise intensities used in this thesis are given in Table 3.3. Due to the lack of data to estimate the noise parameters, these values are selected arbitrarily, with the constraint that the resulting substrate concentration profiles exhibit strictly decreasing behavior. The validation of this proposed noise model and its parameters based on experimental data does not fall within the scope of this work and, therefore, can be conducted as a separate study,

Table 3.3: Maximum noise intensities

Component	Value
Active biomass $\sigma_{X_a,max}$	0.05 $1/\sqrt{h}$
Inactive biomass $\sigma_{X_i,max}$	0.05 $1/\sqrt{h}$
Ammonia $\sigma_{N,max}$	0.01 $1/\sqrt{h}$
Sucrose $\sigma_{Suc,max}$	0.05 $1/\sqrt{h}$
Fructose, Glucose $\sigma_{FG,max}$	0.05 $1/\sqrt{h}$
Malic acid $\sigma_{P,max}$	0.05 $1/\sqrt{h}$

where other noise models can also be considered. Figure 3.4 shows one sample scenario of the stochastic model using the listed noise parameters. This scenario illustrates, in particular, that the nitrogen is depleted earlier than in the deterministic model, resulting in the cessation of active biomass growth. Another difference is evident in the later depletion of sucrose, which results in a delay in the consumption of monosaccharides compared to the deterministic case. Fructose and glucose are also consumed at a seemingly slower rate, as these components are not yet fully depleted at the terminal time step of the simulation in this scenario.

Multiple realizations of the stochastic model can be simulated in Julia by defining an ensemble problem, for which a statistical summary consisting of the mean and variance at each time step is provided. The Euler-Maruyama solver is chosen for the simulation. Figure 3.5 illustrates the summary of an ensemble Julia problem consisting of the averaged concentration profile of the simulated scenarios (depicted with solid lines) and a shaded region representing the 5th to 95th percentile range of the scenario distribution. It is demonstrated that the averaged concentration profiles do not necessarily align with the deterministic model (shown in dashed lines), and that the concentrations from the stochastic model are distributed over a range of values. This observation suggests that different results may be obtained when the models are applied for further analysis, such as for optimization or process control purposes. The difference between the stochastic scenarios and the deterministic model can be attributed to the interplay between the model's nonlinearities and the noise. This interplay can be described using Jensen's inequality, which states that the mean of a nonlinear function g of a random variable X is not equal to the function of the expected value itself [13, 28].

$$\mathbb{E}[g(X)] \begin{cases} \geq g(\mathbb{E}[X]) & \text{for convex } g, \\ \leq g(\mathbb{E}[X]) & \text{for concave } g. \end{cases} \tag{3.35}$$

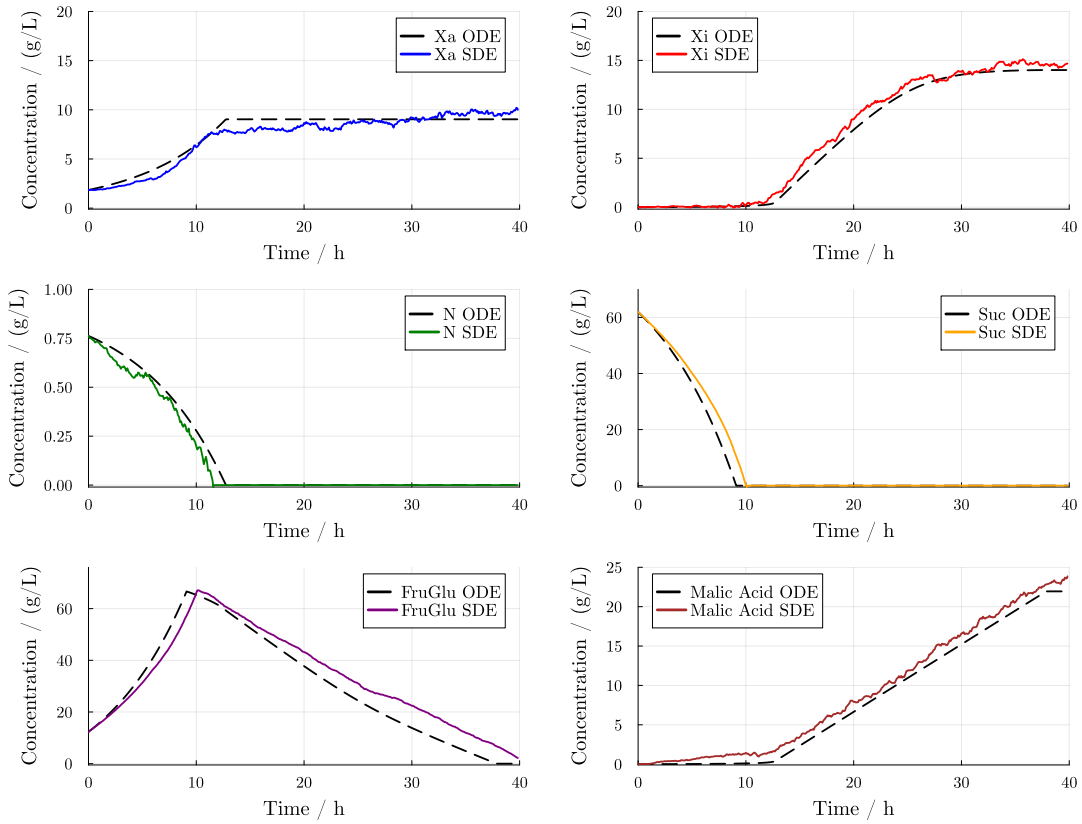

Figure 3.4: Comparison between a scenario of the stochastic model (solid lines) and the deterministic model (dashed lines). From top to bottom, left to right: active biomass, inactive biomass, nitrogen, sucrose, monosaccharides (fructose and glucose), malic acid.

In the bioprocess model, the mean of the stochastic scenarios corresponds to $\mathbb{E}[g(X)]$. In contrast, the deterministic model is the function of the expected value $g(\mathbb{E}[X])$. The dependence of the noise on the time-varying state variables may also contribute to the discrepancy between the SDE average and the expected value given by the ODE solution. This can be seen in the increasing size of the shaded region over time in all reaction species.

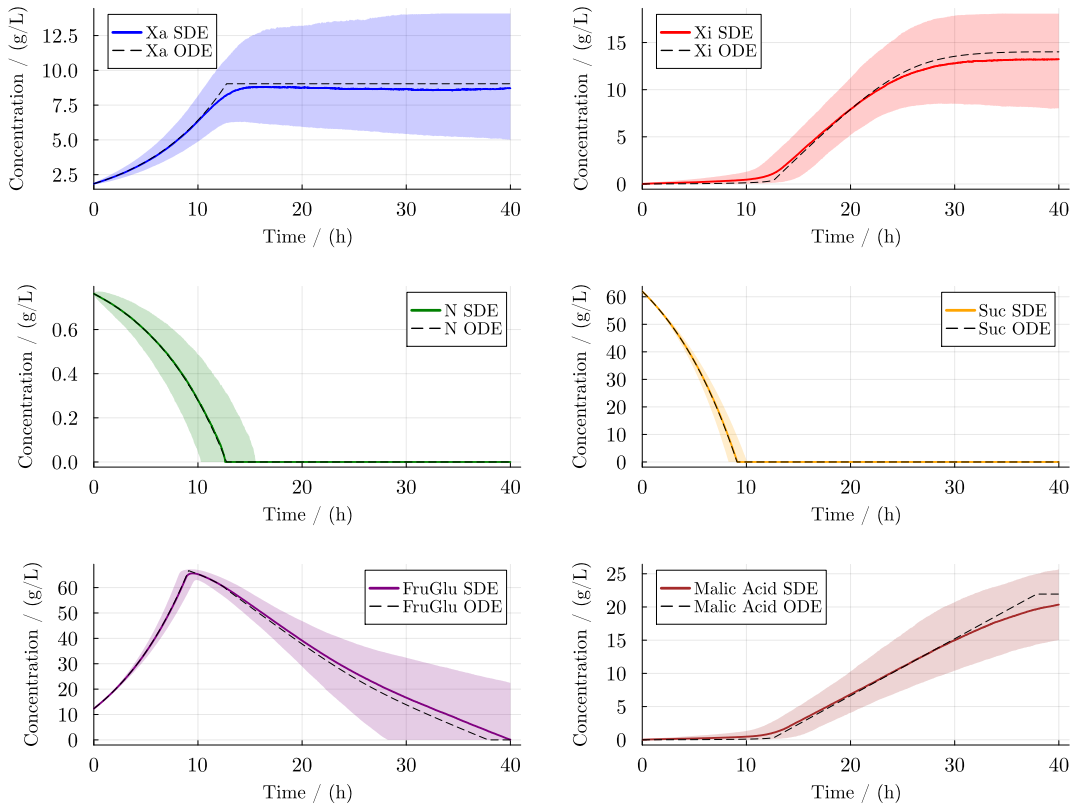

Figure 3.5: SDE Summary of several simulated scenarios consisting of the averaged concentration profile (solid line) and the 5th to 95th percentile of the scenario distribution (shaded region). From top to bottom, left to right: active biomass, inactive biomass, nitrogen, sucrose, monosaccharides (fructose and glucose), malic acid.

4 Optimal Stopping of Bioprocesses

After laying the groundwork on the case study of batch production of malic acid and optimal stopping, this chapter formulates the optimal stopping problem based on this process. The Longstaff-Schwartz algorithm is then applied to learn the optimal stopping rule when the substrate reaches a certain threshold. The results are then presented and discussed.

4.1 Problem Formulation

The goal of the optimal stopping study in this thesis is to determine when the substrate is nearly depleted during the malic acid batch process, when it is modeled as a stochastic process. Formally, we define the minimum threshold

$$\epsilon = 0.05 \cdot (Suc(t_0) + FruGlu(t_0)), \tag{4.1}$$

and the stopping time is defined as the time when the substrate component $FruGlu$ reaches this threshold.

For this thesis, two sets of simulations are conducted, each comprising five thousand scenarios. The simulation sets shall henceforth be referred to as Simulation Set 1 and Simulation Set 2. Figure 4.1 shows the concentration of $FruGlu$ over time, averaged over all scenarios in the ensemble problem of Simulation Set 1. The shaded region represents the 5th to 95th percentile of the concentration distribution in each time step. As illustrated in Figure 4.1, the stochastic reaction model reaches this minimum threshold across a broad range of times, indicating significant variability in the process. Therefore, a stopping rule is necessary to narrow down the optimal time when the substrate nears the depletion point. This stopping time may also be interpreted as an intervention point at which additional substrate may be given to maintain the process.

A significant observation is that, on average, the stochastic scenarios intersect the threshold line later than the deterministic model. This can be explained by the fact that at the final time step, there are scenarios where the concentration of $FruGlu$ remains significantly above the threshold, which skews the average toward later times.

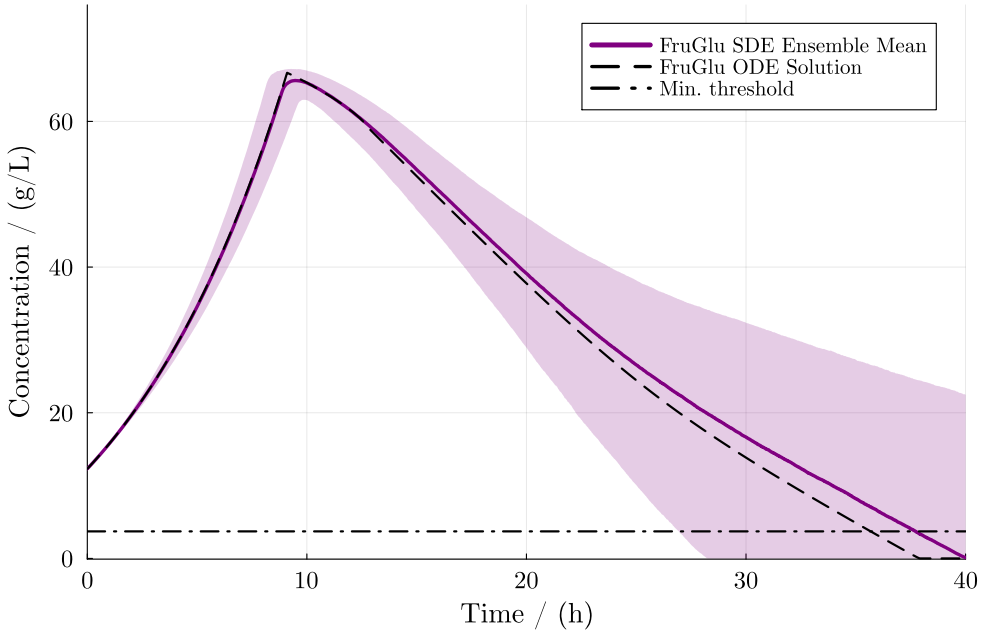

Figure 4.1: SDE summary of the simulated scenarios for $FruGlu$ and the minimum threshold.

From this problem setting, the reward function can be defined as

$$G(t) = -(FruGlu(t) - \epsilon)^2. \tag{4.2}$$

The reward function is formulated in this way to ensure that the maximum is reached when $FruGlu = \epsilon$. From the reward function (4.2), the finite-horizon optimal stopping problem is given as

$$V_* = \sup_{\tau \in [0,T]} \mathbb{E}[-(FruGlu(\tau) - \epsilon)^2]. \tag{4.3}$$

After formulating the problem, the Longstaff-Schwartz algorithm can then be applied. It can be seen in Figure 4.1 that there are scenarios where $FruGlu$ is still significantly above the threshold at the terminal time step. Stopping early does not make sense in these cases because the stopping criteria would not be satisfied before termination.

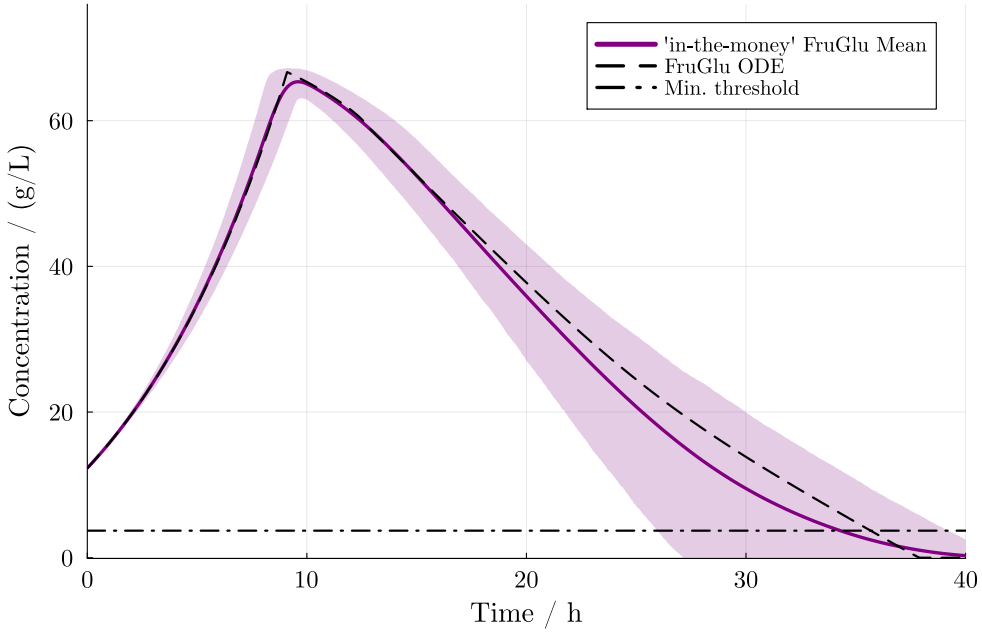

Figure 4.2: SDE summary of the 'in-the-money' $FruGlu$ scenarios and the minimum threshold.

The Longstaff-Schwartz algorithm only considers ITM scenarios, which, in the context of the batch process problem, means that $FruGlu < \epsilon$. This is done so that only scenarios where early stopping is relevant are considered [22]. By filtering out OTM scenarios ($FruGlu > \epsilon$) at the terminal time step, 2,934 scenarios remain from Set 1 and 3,006 scenarios remain from Set 2. The analysis will proceed using these remaining scenarios, as they are the scenarios that can fulfill the stopping criteria before termination in the batch process problem, i.e., the scenarios where the minimum threshold would have been reached before the predefined termination point. The summary of the ITM scenarios from Set 1 is shown in Figure 4.2. In contrast to the summary of all simulated scenarios in Figure 4.1, it can be seen that ITM stochastic scenarios, on average, reach the threshold earlier than the deterministic case. The stochastic scenarios still reach the threshold across a broad range of times. Another important observation is that, at the terminal time step, the shaded region is below the threshold line, which means that even accounting for the variance in the scenarios, the filtered scenarios are, by definition of this problem, the ITM scenarios.

For the following analysis, an equidistant finite time grid $\{t_n = n\Delta t \mid n = 0, 1, \ldots, N\}$ is considered where $t_0 = 0$, $t_N = 40h$, and the interval length is $\Delta t = 0.01h$. This time interval length is also used as the step size of the numerical solver. Following the

discrete time notation, the reward function value at time t_n is denoted as G_n. The terminal time step for the simulation is also the final time of the available experimental data. The conditional expectation is estimated using

$$\mathbb{E}[G_{n+1} \mid \mathcal{F}_n] = \sum_{k=0}^{3} \beta_k \cdot \phi_k(FruGlu(t_n)), \tag{4.4}$$

where $\mathcal{F}_n$ represents the available information up to time t_n. In this case, the information is the concentration of the substrate at time t_n. The first four unweighted Laguerre polynomials are used as basis functions and are given in (4.5)-(4.9). The full Longstaff-Schwartz algorithm for this problem is described in Algorithm 1.

$$\phi_n(x) = \frac{e^x}{n!}\frac{d^n}{dx^n}\left(x^n e^{-n}\right) \tag{4.5}$$

$$\phi_0(x) = 1 \tag{4.6}$$

$$\phi_1(x) = 1 - x \tag{4.7}$$

$$\phi_2(x) = \frac{1}{2}(x^2 - 4x + 2) \tag{4.8}$$

$$\phi_3(x) = \frac{1}{6}(-x^3 + 9x^2 - 18x + 6) \tag{4.9}$$

For comparison, the original example presented by Longstaff and Schwartz used the first four weighted Laguerre polynomials, the general form of which is given in (4.10) [22].

$$\phi_n(x) = \exp(-x/2)\frac{e^x}{n!}\frac{d^n}{dx^n}\left(x^n e^{-n}\right). \tag{4.10}$$

4.2 Results and Discussion

The original Longstaff-Schwartz method yields the optimal exercise boundary for an American option. This exercise rule can then be used to determine the value of an option contract. In this thesis, the viability of the LSMC method is first examined by analyzing the stopping times obtained by applying the algorithm to the formulated optimal stopping problem (4.3). The goal is to determine the time when the substrate component $FruGlu$ reaches a certain lower threshold ϵ. As shown in Figure 4.2, the stochastic model of $FruGlu$ intersects the threshold line across a wide range of time. The distribution obtained directly from the simulations is compared to the

Algorithm 1 Longstaff-Schwartz Algorithm for Batch Process

Require: Stochastic model (3.23)-(3.34), threshold ϵ, reward function G_t,
Require: Finite time horizon $[t_0, t_N]$, step size Δt,
Require: Basis functions ϕ_k (4.6)-(4.9), regression degree K

Define the discrete time grid $\{t_n = n\Delta t \mid n = 0, 1, \ldots, N\}$
Simulate M scenarios of $FruGlu(t)$
Valid paths: $\text{valid\_idx} \leftarrow \{i \mid FruGlu_i(t_N) \leq \epsilon\}$, $M_V \leftarrow \text{length}(\text{valid\_idx})$
Store valid paths: $FG \leftarrow FruGlu_i(t),\ i \in \text{valid\_idx}$ ▷ $FG \in \mathbb{R}^{N \times M_V}$
Calculate reward function: $G \leftarrow G_t(FG_{valid})$ ▷ $G \in \mathbb{R}^{N \times M_V}$
Initialize stopping times: $\tau_i = t_N$ for $i = 1, \ldots, M_V$ ▷ $\tau \in \mathbb{R}^{M_V}$
for n in N-1 to 1 **do**
    ITM paths: $\text{itm\_idx} \leftarrow \{i \in [1, M_V] \mid FG[n, i] \leq \epsilon\}$
    $M_{ITM} \leftarrow \text{length}(\text{itm\_idx})$
    Current state: $FG_n \leftarrow FG[n, \text{itm\_idx}]$
    Immediate reward: $G_n \leftarrow G[n, \text{itm\_idx}]$
    Future reward: $G_{n+1} \leftarrow G[n+1, \text{itm\_idx}]$
    Basis matrix $\mathbf{\Phi}_n$: $\Phi_{n,jk} = \phi_{k-1}(FG[n, j]),\ j \in [1, M_{ITM}],\ k \in [1, K+1]$
    ▷ $\mathbf{\Phi} \in \mathbb{R}^{M_{ITM} \times (K+1)}$
    Least squares regression: $\beta_n \in \arg\min_\beta \|\mathbf{G_{n+1}} - \mathbf{\Phi_n}\beta\|^2$ ▷ $\beta \in \mathbb{R}^{K+1}$
    Conditional expectation: $\mathrm{E}_n = \mathbf{\Phi_n}\beta$
    for each $j \in [1, M_{ITM}]$ **do**
        if $G_n \geq E_n$ **then**
            Update stopping time: $\tau[j] \leftarrow \min(n, \tau[j])$
        else
            Carry forward: $G[n, j] \leftarrow G[n+1, j]$
        end if
    end for
end for

distribution of stopping times resulting from the LSMC algorithm. The ideal outcome would be if the two distributions are similar to each other, which means that the Longstaff-Schwartz algorithm correctly identifies the time when the substrate reaches the threshold by solving the optimal stopping problem. As mentioned in the previous section, two sets of simulations are conducted in this work. The following discussion first focuses on the results obtained from Simulation Set 1. The result from Simulation Set 2 is presented at the end for comparison.

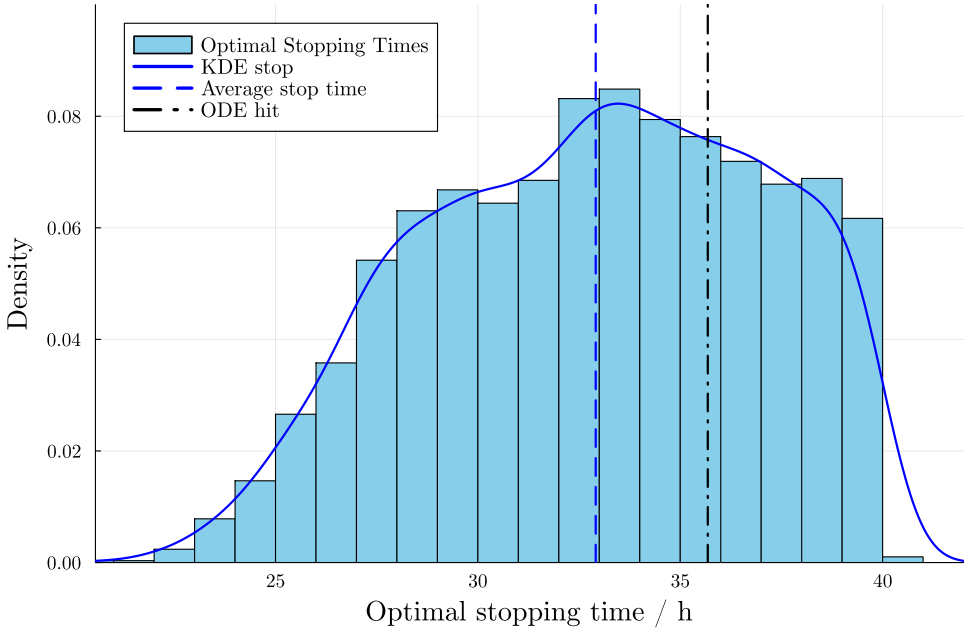

Figure 4.3: Distribution of the optimal stopping times from the Longstaff-Schwartz algorithm and the kernel density estimation (KDE) from Simulation Set 1.

First, the distribution of the stopping times obtained from the Longstaff-Schwartz algorithm is analyzed. Figure 4.3 shows the histogram of the optimal stopping times and the kernel density estimation (KDE) of the distribution from Simulation Set 1. Julia automatically selects the bin length for the histogram, and Gaussian kernels are used for the KDE, where the bandwidth is chosen using Silverman's rule, as per the default settings in Julia's KernelDensity package. The histogram and KDE reveal a unimodal distribution, with the highest density at 33.457 hours. The average stopping time from the LSMC algorithm is 32.911 hours, which is significantly earlier than the time the deterministic model reaches the threshold, which is at 35.68 hours.

The distribution of the optimal times is then cross-referenced with the distribution of the actual times when the stochastic scenarios reach the threshold, henceforth

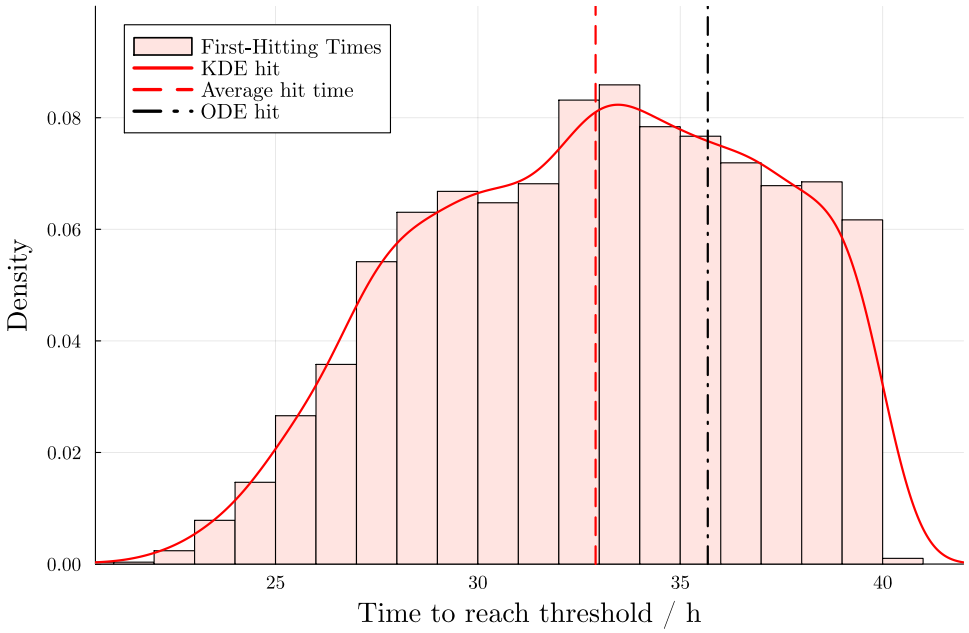

Figure 4.4: Distribution of the first time when $FruGlu$ reaches the minimum threshold and the kernel density estimation (KDE) from Simulation Set 1.

referred to as the 'first hitting time', which is shown in Figure 4.4. The histogram and the KDE also reveal a unimodal distribution with highly similar statistics to the distribution of the optimal stopping times. On average, the stochastic scenarios reach the substrate threshold after 32.908 hours, which corresponds to a difference of less than one minute from the optimal stopping distribution. The same applies to the mode of the distribution, where the highest density is found at 33.47 hours, compared to the 33.46 hours of the optimal stopping distribution.

The average optimal stopping and the first hitting time correspond well to the ensemble summary of the ITM scenarios used in the optimal stopping analysis shown in Figure 4.2, which shows that the average profile of the stochastic scenarios intersects the threshold line at an earlier time in contrast to the deterministic model. The fact that the deterministic model reaches the threshold later than the stochastic optimal stopping time highlights the impact of random fluctuations. As explained in the previous chapter, the difference between the deterministic profile and the average of the stochastic scenarios can be attributed to Jensen's inequality and the accumulation of variability resulting from the dependence of the noise on the state variable. These fluctuations lead to earlier stopping decisions under uncertainty, reflecting risk aversion and opportunistic decision-making embedded in the LSMC algorithm, which takes the

optimal stopping time as the earliest time when the immediate payoff is greater than or equal to the conditional expectation.

To further verify that the LSMC algorithm yields a distribution similar to the actual first hitting times, a two-sample Kolmogorov–Smirnov (KS) test is conducted using Julia's HypothesisTests package. The two-sample KS test is a nonparametric test to determine if two one-dimensional probability distributions differ from each other [29]. The test is performed by comparing the cumulative distributions (CDFs) under the null hypothesis that the two samples are drawn from the same distribution. The underlying cumulative distributions are shown in Figure 4.5. The KS test computes the maximum difference between the two CDFs and tests whether this difference is statistically significant. From the 2,934 scenarios used in the optimal stopping analysis, the test in Julia yields a KS statistic of 0.001363, indicating that the absolute maximum difference between the CDFs is approximately 0.14%. The two-sided p-value in this case is 1, which concludes that the test fails to reject the null hypothesis, even with a large sample size. Failing to reject the null hypothesis indicates that the two distributions are statistically similar, suggesting a substantial equivalence between the results from the LSMC algorithm and the actual first hitting times. It can be concluded that the Longstaff-Schwartz method is a viable option in dealing with stochastic processes in biochemical engineering.

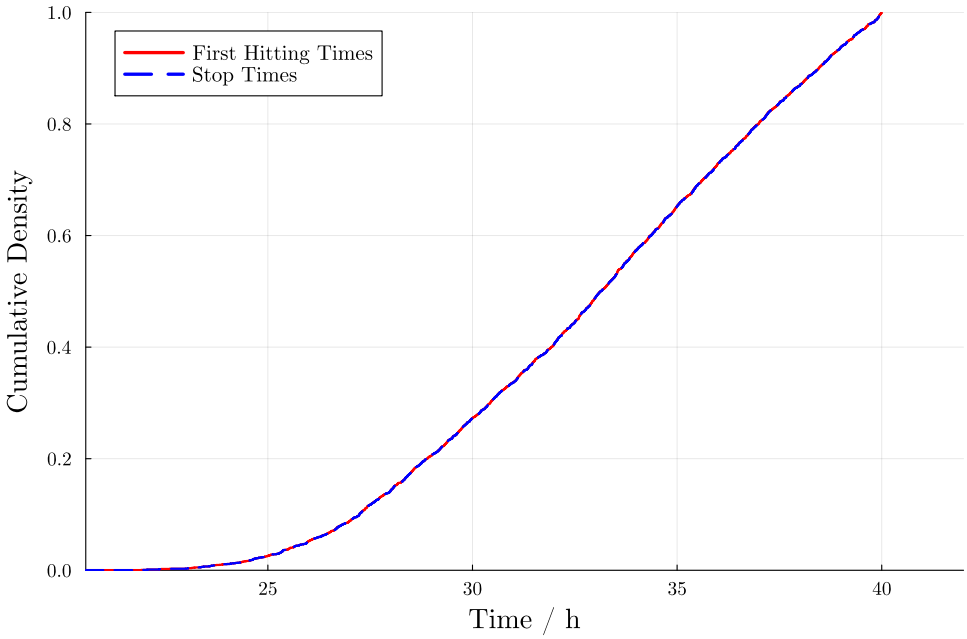

Figure 4.5: Cumulative distribution function (CDF) of the first hitting times and the optimal stopping times from Simulation Set 1.

Validation against another set of simulations

After analyzing the results from the LSMC algorithm on Simulation Set 1, the results from Simulation Set 2 are presented. The LSMC algorithm is then applied to Set 2 to validate the stopping strategy identified in Set 1. However, Simulation Set 2 yields a different distribution of both optimal stopping and first hitting times compared to Simulation Set 1, which is shown in Figure 4.6. The KDE reveals a multimodal distribution of the optimal stopping and first hitting times obtained from Simulation Set 2, where the highest densities are found at 31.83, 35.37, and 37.93 hours. Simulation Set 1 yields a unimodal distribution with a mode of 33.47 hours. On average, the ITM scenarios from Set 2 reach the threshold after 32.96 hours, which is also the average optimal stopping time. This average differs, although not significantly, from the value obtained from Set 1, which is 32.91 hours. The KS test still indicates that the resulting distributions from Simulation Set 2 are statistically similar to each other. The results suggest the need for a sensitivity analysis of the stopping times to grasp the connection between the number of simulations and the resulting distribution.

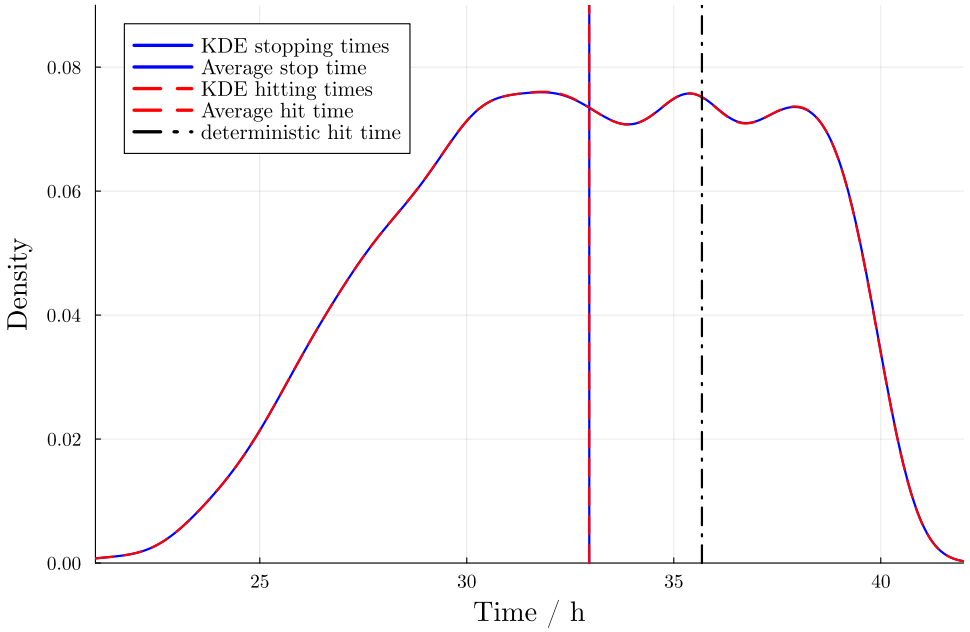

Figure 4.6: KDE of the optimal stopping and first hitting times from Simulation Set 2

Implications of ITM Scenario Selection

Furthermore, an analysis is done to show the significance of filtering out OTM scenarios. Longstaff and Schwartz argue that considering only ITM scenarios leads to a better estimation of the conditional expectation [22]. Figure 4.7 shows the KDEs of the first hitting and the optimal stopping times from Simulation Set 2. The difference here is that, at every step of the backward induction, no ITM selection is applied. The optimal stopping times reveal a significantly different distribution compared to the actual first hitting times, with an average of 32.62 hours, which is even earlier than the average first hitting time.

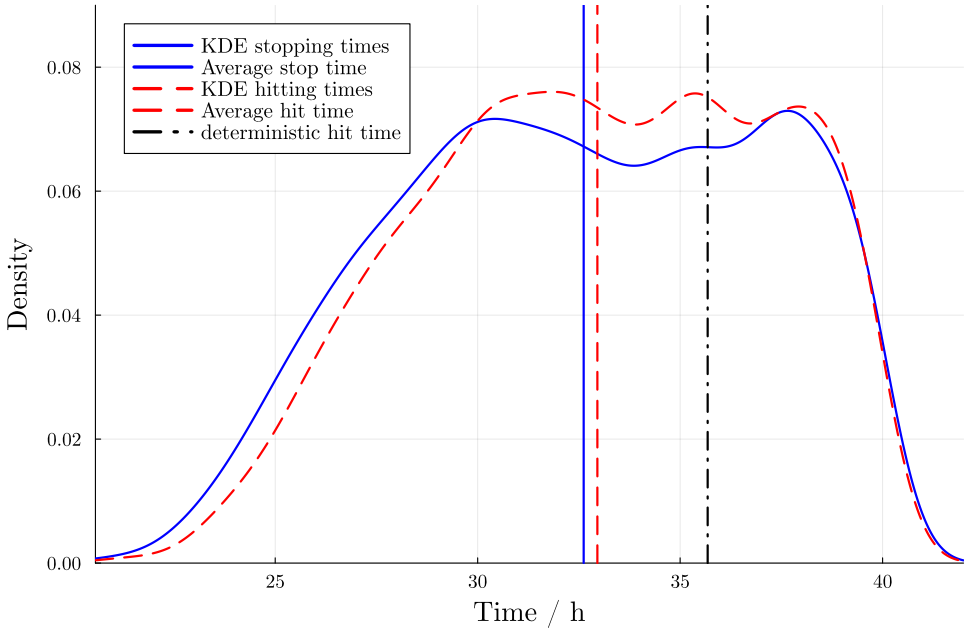

Figure 4.7: KDE of the optimal stopping and first hitting times from Simulation Set 2, without ITM scenario selection.

The statistical difference between the two distributions is further confirmed by performing a two-sample KS test on the two distributions. The KS statistic is found to be 0.0479, indicating that the absolute maximum vertical distance between the CDFs is 4.79%. With a two-sided p-value of 0.002, the KS test rejects the null hypothesis, indicating that the distributions of the first hitting times and the optimal stopping times without ITM filtering are statistically different. This analysis reveals that the LSMC algorithm fails to identify the optimal stopping times accurately when ITM filtering is not applied. This result is expected, as focusing solely on in-the-money (ITM)

scenarios yields a more accurate estimate of the conditional expectation, in line with the approach by Longstaff and Schwartz [22].

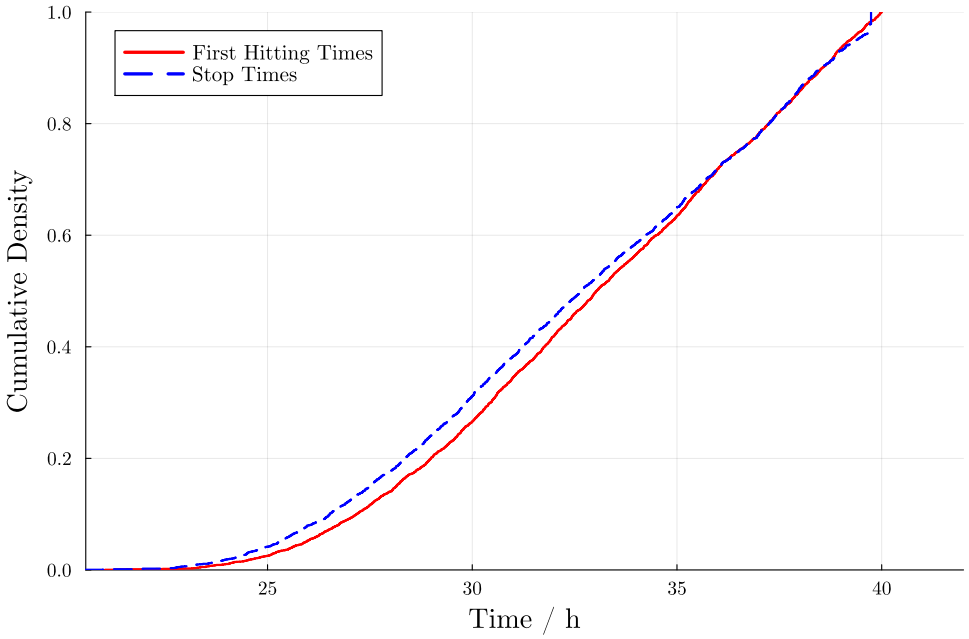

Figure 4.8: CDF of the first hitting times and optimal stopping times without ITM filtering from Simulation Set 2.

5 Summary and Outlook

5.1 Summary

This thesis explored the application of stochastic modeling and optimal stopping theory to biochemical batch processes. Deterministic models, although widely used for process optimization and control, often fail to capture the inherent uncertainties present in biological systems. By extending deterministic models to stochastic differential equations (SDEs), this work accounts for fluctuations in reaction kinetics of biological systems.

A case study was presented involving a stiff biochemical reaction model that describes the batch production of the platform chemical malic acid using *Ustilago trichophora* under nitrogen limitation. The deterministic model was refined through parameter estimation using experimental data and implemented in the programming language Julia. The model was then extended to an SDE framework by introducing noise terms, which are assumed to resemble the Monod kinetics describing the dependence of the metabolic activities of the biomass on substrate availability. Simulation results demonstrated that stochastic dynamics resulted in a distribution of possible process trajectories that diverged from deterministic expectations, underscoring the importance of uncertainty-aware modeling in bioprocess design and control.

To demonstrate the practical value of stochastic modeling, the thesis formulated an optimal stopping problem based on substrate depletion, inspired by techniques in financial mathematics, particularly the valuation of American options. The Longstaff-Schwartz (LSMC) algorithm was adapted and applied to determine the optimal time to intervene in the batch process based on a predefined substrate threshold. The distribution of optimal stopping times obtained from the LSMC method was found to statistically match the actual first hitting times of the threshold, as confirmed by a two-sample Kolmogorov–Smirnov test. Furthermore, the algorithm demonstrated robustness across

two independently generated simulation sets, although variations in distribution shapes suggest the need for sensitivity analysis and larger ensembles in future studies. These findings underscore the viability of methods from financial mathematics in optimizing noisy biochemical processes. The integration of stochastic modeling with simulation-based optimization opens new pathways for risk-aware decision-making in bioprocess operations.

5.2 Outlook

The results from this work lay a good groundwork for adapting methods from financial mathematics to chemical engineering problems containing stochastic dynamics. However, before applying optimization methods, the modeling of the stochastic process should be emphasized, as the optimization framework relies heavily on the SDE model. In this thesis, the inherent noise in a biochemical process is assumed to follow the Monod model, which captures the substrate-dependence of the process. The SDE model proposed in this thesis also assumes that the noise in all reaction species is identical. Future work may focus on validating the proposed noise model and parameters with real process data. Another modeling avenue that could be explored in this regard is the introduction of independent or even correlated BMs as noise generators for each of the species.

The resulting distributions of stopping times from several simulation sets presented in this thesis reveal that the stopping rule from the LSMC might be affected by the underlying simulations. The results suggest the need for a sensitivity analysis of the stopping times to quantify the effect of the number of simulations on the resulting distribution. This analysis aims to determine whether the distributions resulting from multiple simulation sets differ from one another after a specified number of simulated scenarios.

Extending the analysis to continuous or fed-batch systems and exploring real-time control strategies may also be considered as potential avenues for development. Analyzing a continuous system would be a step towards scaling up the production process from a laboratory to an industrial scale. The goal of a continuous system analysis would be to gain insights into the implications of stochastic dynamics in large-scale production. In such an analysis, the optimal stopping problem could consider using a control variable

that can be continuously measured throughout the process. This analysis could yield an actual control strategy based on stochastic dynamics.

Furthermore, to further highlight the consequences of using stochastic models instead of deterministic models in process operation, a techno-economic analysis (TEA) can be conducted. Concrete process design based on stochastic models should identify any differences in process equipment compared to classical process design. TEA can also provide insights into the financial advantages of modeling biochemical processes as a stochastic process. Another possible work based on financial advantage could also involve formulating an optimal stopping problem in terms of monetary gain. In this case, the optimal stopping time can be interpreted as the point at which the process must be stopped to incur the minimum operational cost or the maximum profit, depending on the product yield.

Nomenclature

Abbreviations

BFGS	Broyden-Fletcher-Goldfarb-Shanno
BM	Brownian Motion
CDF	Cumulative Distribution Function
GBM	Geometric Brownian Motion
ITM	In the Money
KDE	Kernel Density Estimation
KS	Kolmogorov-Smirnov
LSMC	Least Squares Monte Carlo
ODE	Ordinary Differential Equation
OTM	Out of the Money
pyFOOMB	Python Framework for Object-Oriented Modeling of Bioprocesses
SDE	Stochastic Differential Equation
TEA	Techno-Economic Analysis

Functions

$\mathbb{E}[X \mid Y]$	Conditional expectation of X given Y
$\mathbb{E}[X]$	Expectation of X
$\mathcal{F}_t$	Information up to time t

$\mathcal{N}(\mu, \sigma^2)$	Normal distribution with mean μ and variance σ^2	
ξ_t	White noise	
B_t	Brownian motion	
G_t	Reward function	
V_t	Value function	

Variables

τ	Optimal stopping time	$[h]$
$FruGlu$	Fructose and Glucose total concentration	$[g/L]$
N	Ammonia concentration	$[g/L]$
P	Malic acid concentration	$[g/L]$
Suc	Sucrose concentration	$[g/L]$
X_a	Active biomass concentration	$[g/L]$
X_i	Inactive biomass concentration	$[g/L]$

Bibliography

[1] J. Almquist, M. Cvijovic, V. Hatzimanikatis, J. Nielsen, and M. Jirstrand. "Kinetic models in industrial biotechnology – Improving cell factory performance". In: *Metabolic Engineering* 24 (2014), pages 38–60. ISSN: 1096-7176. DOI: 10.1016/j.ymben.2014.03.007.

[2] M. D. Graham and J. B. Rawlings. *Modeling and Analysis Principles for Chemical and Biological Engineers*. Santa Barbara: Nob Hill Publishing, 2022. ISBN: 9780975937761.

[3] D. G. Spiller, C. D. Wood, D. A. Rand, and M. R. White. "Measurement of single-cell dynamics". In: *Nature* 465 (7299 June 2010), pages 736–745. ISSN: 00280836. DOI: 10.1038/nature09232.

[4] D. Pischel, K. Sundmacher, and R. J. Flassig. "Efficient simulation of intrinsic, extrinsic and external noise in biochemical systems". In: *Bioinformatics* 33 (14 July 2017), pages i319–i324. ISSN: 14602059. DOI: 10.1093/bioinformatics/btx253.

[5] S. Lisci, M. Grosso, and S. Tronci. "Different Control Strategies for a Yeast Fermentation Bioreactor". In: *IFAC-PapersOnLine*. Volume 54. Elsevier B.V., June 2021, pages 306–311. DOI: 10.1016/j.ifacol.2021.08.259.

[6] P. R. Patnaik. "External, extrinsic and intrinsic noise in cellular systems: analogies andimplications for protein synthesis". In: *Biotechnology and Molecular Biology Review* 1 (4 2006), pages 121–127. ISSN: 1538-2273. URL: http://www.academicjournals.org/BMBR.

[7] M. Thattai and A. V. Oudenaarden. "Intrinsic Noise in Gene Regulatory Networks". In: *Proceedings of the National Academy of Sciences*. 2001, pages 8614–8619. DOI: 10.1073/pnas.151588598. URL: www.pnas.orgcgidoi10.1073pnas.151588598.

[8] D. T. Gillespie. "Stochastic Simulation of Chemical Kinetics". In: *Annual Review of Physical Chemistry* 58 (2007), pages 35–55. ISSN: 0066426X. DOI: 10.1146/annurev.physchem.58.032806.104637.

[9] S. Shreve. *Stochastic Calculus for Finance I: The Binomial Asset Pricing Model*. Springer-Verlag, 2004. ISBN: 9780387225272. DOI: 10.1007/978-0-387-22527-2.

[10] N. Freeman and R. Stephenson. *Stochastic Processes and Financial Mathematics*. University of Sheffield, 2025. URL: https://nicfreeman1209.github.io/Website/MASx52/index.html.

[11] Committee on Balance of Payment Statistics. *Financial Derivatives*. International Monetary Fund, Oct. 1998.

[12] N. Privault. *Introduction to Stochastic Finance with Market Examples*. 2nd. Chapman and Hall/CRC, 2022. DOI: 10.1201/9781003298670.

[13] U. H. Thygesen. *Stochastic Differential Equations for Science and Engineering*. New York: Chapman & Hall/CRC, 2023. DOI: 10.1201/9781003277569.

[14] P. Glasserman. *Monte Carlo Methods in Financial Engineering*. Springer, 2003. DOI: 10.1007/978-0-387-21617-1.

[15] R. Durrett. *Probability: Theory and Examples*. Cambridge University Press, Apr. 2019. ISBN: 9781108591034. DOI: 10.1017/9781108591034.

[16] S. Särkkä and A. Solin. *Applied Stochastic Differential Equations*. Cambridge University Press, 2019. DOI: 10.1017/9781108186735.

[17] B. Øksendal. *Stochastic Differential Equations: An Introduction with Applications*. 5th edition. Springer, 2000.

[18] A. Shiryaev and G. Peskir. *Optimal Stopping and Free-Boundary Problems*. Birkhäuser Verlag, 2006. ISBN: 3764324198. DOI: 10.1007/978-3-7643-7390-0.

[19] R. Bellman. *Dynamic programming*. Princeton University Press, 1957. ISBN: 069107951X.

[20] J. F. Carriere. "Valuation of the early-exercise price for options using simulations and nonparametric regression". In: *Insurance: Mathematics and Economics* 19 (1996), pages 19–30. DOI: 10.1016/S0167-6687(96)00004-2.

[21] J. N. Tsitsiklis and B. V. Roy. "Optimal Stopping of Markov Processes: Hilbert Space Theory, Approximation Algorithms, and an Application to Pricing High-Dimensional Financial Derivatives". In: *IEEE Transactions on Automatic Control* 44 (10 1999). DOI: 10.1109/9.793723.

[22] F. A. Longstaff and E. S. Schwartz. "Valuing American Options by Simulation: A Simple Least-Squares Approach". In: *The Review of Financial Studies* 14.1 (June 2015), pages 113–147. ISSN: 0893-9454. DOI: 10.1093/rfs/14.1.113.

[23] H. Fogler. *Elements of Chemical Reaction Engineering*. International Series in the Physical and Chemical Engineering Sciences. Pearson Education, 2020. ISBN: 9780135486269.

[24] J. Monod. "The Growth of Bacterial Cultures". In: *Annual Review of Microbiology* 3.1 (Oct. 1949), pages 371–394. ISSN: 1545-3251. DOI: 10.1146/annurev.mi.03.100149.002103.

[25] M. Maschmeier. "Modeling of the Fermentation Kinetics of the Platform Chemical Malic Acid under Secondary Substrate Limitation". RWTH Aachen University, Apr. 2024.

[26] W. Dahmen and A. Reusken. *Numerik für Ingenieure und Naturwissenschaftler*. Springer Berlin Heidelberg, 2008. ISBN: 978-3-540-76492-2. DOI: 10.1007/978-3-540-76493-9.

[27] G. Bärwolff. *Numerik für Ingenieure, Physiker und Informatiker*. Springer Berlin Heidelberg, 2016. DOI: 10.1007/978-3-662-48016-8.

[28] A. Nobel. *Convex Functions and Jensen's Inequality*. Sept. 2024. URL: https://nobel.web.unc.edu/teaching/stor-555-theoretical-statistics/stor-555-lecture-notes/.

[29] T. Soong. *Fundamentals of Probability and Statistics for Engineers*. John Wiley & Sons Ltd, 2004. ISBN: 0-470-86814-7.

List of Figures

List of Tables